

Identification and Functional Analysis of a Novel Osteoclastogenesis
Regulator, Siglec-15

A Dissertation Submitted to
the Graduate School of Life and Environmental Sciences,
the University of Tsukuba
in Partial Fulfillment of the Requirements
for the Degree of Doctor of Philosophy in Biological Science
(Doctoral Program in Biological Sciences)

Yoshiharu HIRUMA

Table of Contents

Abstract.....	1
Abbreviations	4
General Introduction.....	6
Chapter 1	
Identification of Siglec-15, a Member of the Sialic Acid-Binding Lectin, as a Novel Regulator for Osteoclast Differentiation	
Summary.....	12
Introduction	13
Materials and Methods	15
Results	22
Discussion.....	33
Chapter 2	
Impaired Osteoclast Differentiation and Function and Mild Osteopetrosis Development in Siglec-15-deficient Mice	
Summary.....	37
Introduction	38
Materials and Methods	41
Results	47
Discussion.....	59
General Discussion	63
Acknowledgements	69
References	70

Abstract

Bone is a dynamic tissue being continuously remodeled by the coordinated actions of the bone resorbing osteoclasts and bone forming osteoblast lineage cells. This bone turnover is essential to maintain bone strength and mineral homeostasis, and an imbalance between bone formation and resorption—an increased activity of osteoclasts compared to osteoblasts—leads to osteoporosis, which represents a net loss of bone mass and ultimately an increased fracture risk. Although multiple antiresorptive agents which inhibit the activity of osteoclasts and reduce bone resorption have been developed, there is still an unmet medical need for creating new agents for the treatment of osteoporosis that provide enough reduction in the risk of fractures, and also provide long-term safety with less concerns about adverse effects of the treatment. I started my current studies in order to identify novel genes involved in the function of osteoclasts and to validate them as new molecular targets for anti-osteoporosis drugs. As a result of *in silico* screening using a human gene expression database, I found sialic acid-binding immunoglobulin-like lectin 15 (Siglec-15) to be one of the genes markedly overexpressed in giant cell tumor of bone which is a locally aggressive intraosseous neoplasm and characterized by clinical findings of osteolytic bone destruction. The mRNA expression level of Siglec-15 increased in association with osteoclast differentiation in cultures of mouse primary unfractionated bone marrow cells (UBMC), RAW264.7 cells of the mouse macrophage cell line, and human osteoclast precursors (OCP), indicating this gene's relationship with osteoclast differentiation. Treatment with polyclonal antibody to mouse Siglec-15 markedly inhibited osteoclast differentiation in primary mouse bone marrow-derived monocyte/macrophage (BMM) cells stimulated

with the receptor activator of nuclear factor κ B ligand (RANKL) or tumor necrosis factor- α (TNF- α). The antibody also inhibited osteoclast differentiation in cultures of mouse UBMC and RAW264.7 cells stimulated with active vitamin D₃ and RANKL, respectively. Similarly to mouse cells, treatment with polyclonal antibody to human Siglec-15 inhibited RANKL-induced tartrate-resistant acid phosphatase (TRAP)-positive multinuclear cell formation in human OCP cultures. These results suggest an important role of Siglec-15 in mouse and human osteoclast differentiation and the potential use of antibody targeting Siglec-15 for treating bone disorders related to increased osteoclast activity. To discern the physiological role of Siglec-15 in skeletal development and osteoclast formation and/or function *in vivo*, I generated Siglec-15-deficient (*Siglec15^{-/-}*) mice and analyzed their phenotype. The *Siglec15^{-/-}* mice developed without physical abnormalities other than increased trabecular bone mass in lumbar vertebrae and metaphyseal regions of the femur and tibia, causing mild osteopetrosis. Histological analyses demonstrated that the number of osteoclasts present on the femoral trabecular bone of the mutant mice was comparable to that of the wild-type mice. However, urinary deoxypyridinoline, a systemic bone resorption marker, decreased in the *Siglec15^{-/-}* mice, suggesting that the impaired osteoclast function was responsible for increased bone mass in the mutant mice. In addition, the ability of BMM from the *Siglec15^{-/-}* mice to differentiate into osteoclasts was impaired, as determined *in vitro* by cellular TRAP activity in response to RANKL or TNF- α . These results reveal the importance of Siglec-15 in the regulation of osteoclast formation and/or function *in vivo*, providing new insights into the biology of osteoclasts. The findings in the current

studies will provide new opportunities to develop therapeutics targeting Siglec-15 for the treatment of osteoporosis.

Abbreviations

BMM	bone marrow-derived monocyte/macrophage
CLEC4A	C-type lectin domain family 4, member A
DAP12	DNAX-activating protein of 12 kDa
DPD	deoxypyridinoline
FcR γ	Fc receptor γ subunit
GCT	giant cell tumor of bone
IgLRs	immunoglobulin-like receptors
IL-1	interleukin-1
ITAM	immunoreceptor tyrosine-based activation motif
M-CSF	macrophage colony-stimulating factor
MEGF10	multiple EGF-like-domains 10
NFATc1	nuclear factor of activated T-cells, cytoplasmic, calcineurin-dependent 1
OCP	osteoclast precursors
PLC γ	phospholipase C γ
pQCT	peripheral quantitative computed tomography
RANK	receptor activator of nuclear factor κ B
RANKL	receptor activator of nuclear factor κ B ligand
Siglec-15	sialic acid-binding immunoglobulin-like lectin 15
TNF- α	tumor necrosis factor- α
TRAF6	tumor necrosis factor receptor-associated factor 6
TRAP	tartrate-resistant acid phosphatase
TREM-2	triggering receptor expressed on myeloid cells 2

UBMC unfractionated bone marrow cells

vBMC volumetric bone mineral content

General Introduction

Bone is a dynamic tissue being continuously remodeled by the coordinated actions of the bone resorbing osteoclasts and bone forming osteoblast lineage cells [1]. This bone turnover—resorbing old bone and forming new bone—is essential to maintain bone strength and mineral homeostasis during adulthood. In physiological conditions, the balance between bone formation and resorption is appropriately regulated, and these opposing processes interact to form a functional coupling [2].

Osteoporosis is the most common bone disease in humans representing a major public health problem, and is characterized by low bone mass, compromised bone strength and an increase in the risk of fracture. Osteoporosis is a systemic skeletal disease that results from an imbalance between bone formation and resorption; an increased activity of osteoclasts compared to osteoblasts leads to a net loss of bone mass and ultimately an increased fracture risk. Drugs for osteoporosis treatment are classified as either antiresorptive or anabolic. Antiresorptive agents inhibit the activity of osteoclasts and reduce bone resorption, while anabolic agents activate osteoblasts and stimulate bone formation. Currently in the US, multiple antiresorptive agents are available for the prevention and/or treatment of postmenopausal osteoporosis, which include bisphosphonates, calcitonin, estrogen, selective estrogen receptor modulators, and the receptor activator of nuclear factor κ B ligand (RANKL) inhibitor [3, 4]. Bisphosphonates [5] are the most widely used drugs, owing to their potent effects in inhibiting bone resorption. Recently, concerns of rare but serious complications, such as osteonecrosis of the jaw [6, 7] and atypical femoral fractures [8, 9], have been raised with long-term bisphosphonate use. Although the actual risk of these complications

associated with the use of bisphosphonates remains uncertain, and further studies are needed to clarify their pathogenesis and true incidence rate, it is considered that the dramatic decrease in bone turnover with these potent antiresorptive treatments underlies the cause of such complications. Thus, there is still an unmet medical need for creating new agents for osteoporosis treatment that provide enough reduction in the risk of fractures and also provide long-term safety with less concern of adverse effects.

Osteoclasts are multinucleated cells positive for tartrate-resistant acid phosphatase generated from mononuclear monocyte/macrophage lineage hematopoietic precursors [10], and resorb bone by secreting protons and proteases such as cathepsin K into the resorption lacunae. In functional coupling, osteoblasts regulate osteoclast formation both by secreting factors such as macrophage colony-stimulating factor, interleukin-1 (IL-1), and IL-6 [11], and by direct interaction with osteoclast precursors [12, 13]. Among such osteoblast-derived factors, RANKL is the principal regulator of osteoclastogenesis; RANKL is produced by cells of osteoblastic lineage, and binds to its receptor, the receptor activator of nuclear factor- κ B (RANK) expressed on the cell surface of osteoclast precursors, triggering key intracellular signaling cascades [14-17].

Together with RANKL/RANK signaling, costimulatory signals mediated by immunoreceptor tyrosine-based activation motif (ITAM)-bearing adaptor proteins are required for the terminal differentiation of osteoclasts [18-20] (Fig 1). DNAX-activating protein of 12 kDa (DAP12) is one such ITAM-bearing adaptor; its deficiency is reportedly associated with skeletal abnormalities in mice and humans, suggesting the involvement of this signaling pathway in regulating osteoclast development and/or function [21-25]. ITAM-bearing adaptor proteins have minimal extracellular binding

domains and are thought to convey extracellular signals through interaction with ligand-binding, immunoglobulin-like receptors (IgLRs) (Fig 1). Triggering receptor expressed on myeloid cells 2, signal-regulatory protein β 1, and myeloid DAP12-associating lectin-1 are IgLRs expressed on osteoclasts, and candidate DAP12-associating partners [18, 20, 25]. However, studies in mutant mice have not yet clarified the relevance of these genes in bone homeostasis, implying the existence of undiscovered DAP12-associated receptors critical for osteoclastogenesis.

As described above, extensive research has been clarifying the biology of osteoclasts on the molecular level, and based on these elucidated molecular mechanisms, various therapeutic agents have been developed which are effective for treating osteoporotic patients. However, as the molecular mechanisms regulating osteoclastogenesis are not fully understood, there still remains the possibility of existing undiscovered osteoclast-related molecules. When discovered, such molecules can be new targets for drug development which could fulfill the medical needs that are unmet by current osteoporosis therapies. I started the current studies in order to identify novel genes involved in osteoclastogenesis and to validate them as new molecular targets for anti-osteoporosis drugs.

As a result of *in silico* screening by using a human gene expression database, I found sialic acid-binding immunoglobulin-like lectin 15 (Siglec-15) to be one of the genes markedly overexpressed in giant cell tumor of bone which is a locally aggressive intraosseous neoplasm and is characterized by clinical findings of osteolytic bone destruction [26]. Siglec-15 is a newly identified member of the Siglec family of cell-surface IgLRs that recognizes sialylated glycan ligands [27-30]. The molecule

contains one N-terminal V-set immunoglobulin domain and one C2-set immunoglobulin domain in the extracellular region, and preferentially recognizes Neu5Ac α 2-6GalNAc α -structures (α (2,6)-linked sialic acid) through the V-set domain. Siglec-15 was reported as being expressed on macrophages and/or dendritic cells and is highly conserved throughout vertebrate evolution. In intracellular signaling, Siglec-15 reportedly associates more avidly with DAP12 than other ITAM-bearing signaling adaptors, such as the DNAX-activating protein of 10 kDa or Fc receptor γ subunit, in 293T cells co-transfected with constructs expressing these genes [29]. Although a certain regulatory role in the immune system has been suggested based on its gene expression in macrophages and/or dendritic cells [29], the physiological role of Siglec-15 in vertebrates remains unknown.

In Chapter 1, I demonstrate, based on the expression profiles and functional analysis using polyclonal antibody, that Siglec-15 is crucially involved in osteoclast differentiation *in vitro*. In Chapter 2, I discuss how I generated and analyzed Siglec-15-deficient mice to elucidate the physiological role of this gene *in vivo*, especially during osteoclastogenesis and skeletal development. Finally, in General Discussion, I describe the possibility of the development of a new drug targeting Siglec-15 for the treatment of osteoporosis, and what remains to be clarified in future studies in order to fully understand the physiological role of this molecule in the biology of osteoclasts.

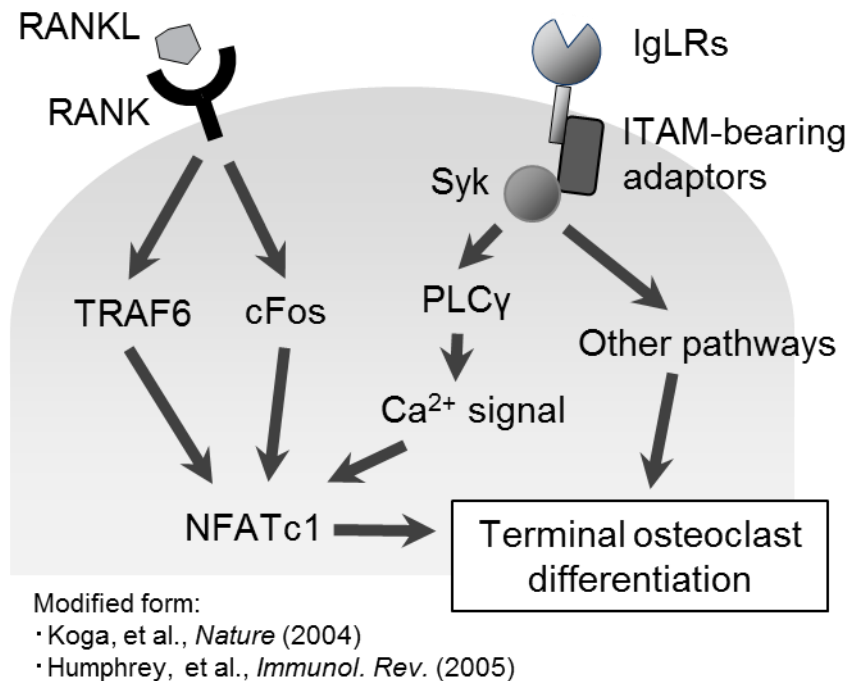


Fig. 1. Current understanding of intracellular signaling required for the terminal osteoclast differentiation. RANKL/RANK signaling mediated by tumor necrosis factor receptor-associated factor 6 (TRAF6) and cFos induces expression of the nuclear factor of activated T-cells, cytoplasmic, calcineurin-dependent 1 (NFATc1), a key transcription factor for osteoclastogenesis. Together with RANKL/RANK signaling, costimulatory signals mediated by ITAM-bearing adaptor proteins are required for the terminal differentiation of osteoclasts. Upon binding to IgLRs, ITAM-bearing adaptors recruit Syk family kinases, leading to the activation of phospholipase C γ (PLC γ) and calcium signaling, which is critical for NFATc1 activation. Syk downstream pathways other than PLC γ /calcium signaling are also important for the terminal osteoclast differentiation.

Chapter 1

Identification of Siglec-15, a Member of the Sialic Acid-Binding Lectin, as a Novel Regulator for Osteoclast Differentiation

Summary

Osteoclasts are tartrate-resistant acid phosphatase (TRAP)-positive multinucleated cells derived from monocyte/macrophage-lineage precursors and are critically responsible for bone resorption. In giant cell tumor of bone (GCT), numerous TRAP-positive multinucleated giant cells emerge and severe osteolytic bone destruction occurs, implying that the emerged giant cells are biologically similar to osteoclasts. To identify novel genes involved in osteoclastogenesis, I searched genes whose expression pattern was significantly different in GCT from normal and other bone tumor tissues. By screening a human gene expression database, I identified sialic acid-binding immunoglobulin-like lectin 15 (Siglec-15) as one of the genes markedly overexpressed in GCT. The mRNA expression level of Siglec-15 increased in association with osteoclast differentiation in cultures of mouse primary unfractionated bone marrow cells (UBMC), RAW264.7 cells of the mouse macrophage cell line and human osteoclast precursors (OCP). Treatment with polyclonal antibody to mouse Siglec-15 markedly inhibited osteoclast differentiation in primary mouse bone marrow-derived monocyte/macrophage (BMM) cells stimulated with receptor activator of nuclear factor κ B ligand (RANKL) or tumor necrosis factor- α (TNF- α). The antibody also inhibited osteoclast differentiation in cultures of mouse UBMC and RAW264.7 cells stimulated with active vitamin D₃ and RANKL, respectively. Finally, treatment with polyclonal antibody to human Siglec-15 inhibited RANKL-induced TRAP-positive multinuclear cell formation in a human OCP culture. These results suggest that Siglec-15 plays an important role in osteoclast differentiation.

Introduction

Osteoclasts are bone-resorbing multinucleated cells generated from mononuclear monocyte/macrophage-lineage hematopoietic precursors. The receptor activator of nuclear factor κ B ligand (RANKL) is the principal regulator of osteoclastogenesis, which binds to its receptor, the receptor activator of nuclear factor κ B (RANK) expressed on the cell surface of osteoclast precursors, and induces osteoclast formation and activation [14-16]. This RANKL/RANK system is not only crucial for physiological osteoclast formation, but also implicated in the pathogenesis of diseases associated with enhanced osteoclastic bone resorption, which include bone destruction in rheumatoid arthritis, bone metastasis of cancer cells and metabolic bone diseases such as postmenopausal osteoporosis [31]. Therefore, it is quite rational to develop therapeutics for treating such disorders by suppressing osteoclastic bone resorption through inhibiting the RANKL/RANK system [32]. However, as the molecular mechanisms regulating osteoclastogenesis are not fully understood, there still remains the possibility of existing undiscovered osteoclast-related molecules which can be new targets for drug development.

Giant cell tumor of bone (GCT) is a locally aggressive intraosseous neoplasm and characterized by clinical findings of osteolytic bone destruction [26]. Its tumoral tissue consists of neoplastic stromal cells, mononuclear histiocytic cells and multinucleated giant cells. Although the origin of GCT is still incompletely understood, it is likely that an osteoclastogenic environment is formed in GCT, since RANKL and RANK have been reported to be overexpressed in the tumor [33-36]. In addition, a number of osteoclast-related genes have been reported to be overexpressed in GCT, including

tartrate-resistant acid phosphatase (TRAP), multiple components of vacuolar-H⁺-ATPase and dendritic cell-specific transmembrane protein [36]. These findings suggest a biological similarity between giant cells that emerged in GCT and normal osteoclasts.

To identify genes involved in osteoclastogenesis and to discover novel drug targets for metabolic bone diseases, I searched genes whose expression level in GCT was significantly different from that in normal and other bone tumor tissues using a human gene expression database. The screening identified sialic acid-binding immunoglobulin-like lectin 15 (Siglec-15) as one of the genes markedly overexpressed in GCT. Siglec-15 is a newly identified member of the Siglecs, which are cell-surface receptors that recognize sialylated glycans [27-29]. Siglec-15 has been reported as being expressed on macrophages and/or dendritic cells and as being highly conserved throughout vertebrate evolution [29]. Although a certain regulatory role in the immune system has been suggested, the physiological role of Siglec-15 in the vertebrate remains unknown. To reveal relationship of this newly identified gene to osteoclastogenesis, I conducted *in vitro* studies using human and mouse osteoclast precursor cells. I demonstrated here, based on the expression profiles and functional analysis using polyclonal antibody, that Siglec-15 is crucially involved in osteoclast differentiation.

Materials and Methods

In silico screening for GCT-related genes

The human gene expression database, BioExpress System (Gene Logic Division, Ocimum Biosolutions, Inc.), containing Affymetrix U133 GeneChip expression profiles of numerous human samples from more than 60 normal and diseased tissue types, was analyzed to identify genes specifically up- or down-regulated in GCT. The gene expression values for each probe set were retrieved from bone samples consisting of 12 GCT samples, 10 tumor samples other than GCT and 7 normal samples using the BioExpress Web Export tool. Genes significantly ($p < 0.05$) up- or down-regulated in the GCT samples compared to the combined set of other tumors and normal samples were determined as GCT-related genes. These genes were further analyzed regarding Pearson's correlation ($|r| > 0.7$) with RANK (Affymetrix ID: 207037_at) or RANKL (210643_at and 211153_s_at) in their expression values by using in-house Perl programs. The TMHMM program [37] was utilized to predict the topology of the gene products.

Cell preparation and culture

Mouse bone marrow-derived monocyte/macrophage (BMM) cells were prepared according to the previously described method with slight modifications [18]. Briefly, bone marrow cells were flushed out from femurs and tibiae of male ddY mice (Japan SLC) and seeded to flasks. After being cultured overnight, non-adherent cells were collected and cultured in 96-well plates (3×10^4 cells/well) in the presence of 5 ng/mL human macrophage colony-stimulating factor (M-CSF) (R&D Systems) for 2 days to

generate mouse BMM. Mouse primary unfractionated bone marrow cells (UBMC) were prepared from mouse femurs and tibiae. RAW264.7 cells were purchased from American Type Culture Collection. Mouse BMM, UBMC and RAW264.7 cells were cultured in α -MEM (Invitrogen) containing 10% fetal bovine serum, 100 μ g/mL streptomycin and 100 U/mL penicillin. Poietics Human Osteoclast Precursors (OCP) were cultured with OCP Basal Medium supplemented with 10% fetal bovine serum, 2 mM L-glutamine, 100 μ g/mL streptomycin and 100 U/mL penicillin (all from Lonza Walkersville) according to the manufacturer's instructions.

Quantitative RT-PCR

RAW264.7 cells were seeded at 4.5×10^5 cells in 75-cm² flasks, and cultured with or without 40 ng/mL human RANKL for 0–3 days. Mouse UBMC was seeded at 5×10^5 cells/well in 96-well plates, and cultured with or without 2×10^{-8} M active vitamin D₃ (Sigma-Aldorich) for 8 days. Human OCP was seeded at 1×10^4 cells/well in 96-well plates, and cultured in medium containing 33 ng/mL M-CSF with or without 53.2 ng/mL RANKL for 3 days. The mRNA expression levels of GCT-related genes, cathepsin K, TRAP and ribosomal protein L32 as an endogenous reference were quantified by the real-time PCR method on a sequence detection system (ABI Prism 7700; Applied Biosystems). Specific primers and probes were used for amplification of mouse genes including CD84 (forward, 5'-ACATGCTCTGTGGAAAAGGAAG-3'; reverse, 5'-GATGGAAGCTTGGAGTGTCTGT-3'; probe, 5'-TACAGCCCAGAACCCTGTCAGCAACAGT-3'), Siglec-15 (forward, 5'-TCAGGCTCAGGAGTCCAATTAT-3'; reverse, 5'-GGTCTAGCCTGGTACTGTCCTTT-3'; probe, 5'-ATTTGAGCCA

GATGAGTCCTCCAGGCCA-3'), multiple EGF-like-domains 10 (MEGF10) (forward, 5'-CTCATCTGCTCACTGCTCTGTC-3'; reverse, 5'-GTAGCTGATTCTGTGCCGTGT-3'; probe, 5'-ACTGGGAAAGCTACTCGGTGACTGTGCA-3'), C-type lectin domain family 4, member A (CLEC4A) (forward, 5'-ATTCTGGCACAATGGTGA GC-3'; reverse, 5'-GAATGCCCATGAAGAATGAGTG-3'; probe, 5'-TTGGAAGACT GGATGGGGCTGGAACGA-3'), cathepsin K (forward, 5'-GGCATCTTTCCAGTTT TACAGC-3'; reverse, 5'-GTTGTTCTTATTCCGAGCCAAG-3'; probe, 5'-ATGTGA ACCATGCAGTGTGGTGGTGGG-3'), TRAP (forward, 5'-GAACTTCCCCAGCCC TTACTAC-3'; reverse, 5'-AACTGCTTTTTGAGCCAGGAC-3'; probe, 5'-TTGCCA GTCAGCAGCCCAAATGCCT-3') and L32 (forward, 5'-AAGAAGTTCATCAGG CACCAGT-3'; reverse, 5'-CTTGACATTGTGGACCAGGAAC-3'; probe, 5'-AAAC CCAGAGGCATTGACAACAGGGTGC-3'). Specific primers and probes were used for amplification of human genes including cathepsin K (forward, 5'-CCGCAG TAATGACACCCTTT-3'; reverse, 5'-AAGGCATTGGTCATGTAGCC-3'; probe, 5'-TCAGGGTCAGTGTGGTTCCTGTTGGGCT-3'), TRAP (forward, 5'-CTGTCCTG GCTCAAGAAACA-3'; reverse, 5'-CCATAGTGGAAGCGCAGATA-3'; probe, 5'-TG AGAATGGCGTGGGCTACGTGCTGAGT-3'), Siglec-15 (forward, 5'-CAGCCACCA ACATCCATTTTC-3'; reverse, 5'-CGCTCAAGCTAATGCGTGTA-3'; probe, 5'-AAGA ACAAAGGCCAGTGCGAGGCTTGGC-3') and L32 (forward, 5'-GAGATCGCTCA CAATGTTTCCT-3'; reverse, 5'-GATGCCAGATGGCAGTTTTTAC-3'; probe, 5'-AC CGCAAAGCCATCGTGGAAGAGCTG-3'). Samples were heated at 50°C for 2 min, 95°C for 10 min and amplified for 40 cycles of 15 sec at 95°C and 1 min at 60°C.

Production of soluble Siglec-15 proteins

Two soluble forms of mouse Siglec-15 protein were produced by fusing the predicted extracellular domain of mouse Siglec-15 (amino acids 1-258) to the Fc region of human IgG1 or to a peptide containing a six-histidine tag. PCR was performed to amplify the extracellular domain of mouse Siglec-15 with the following two primers: 5'-ggggacaagtttgtaaaaaagcaggcttcaccATGGAGGGGTCCCTCCAACCTC-3' and 5'-ggggaccactttgtacaagaagctgggtcTCCGGGGGCGCCGTGGAAGCGGAAC-3'. The PCR product was then inserted into pDONR221 vector (Invitrogen) to generate an entry clone. Siglec-15-Fc or Siglec-15-His protein expression vectors were constructed by recombining the extracellular domain of Siglec-15 from the entry clone into destination vectors, which were designed to add the C-terminal Fc region of human IgG1 (232 amino acids), or a six-histidine tag, respectively. These expression vectors were transfected into FreeStyle 293F cells (Invitrogen) for protein production. The expression of Siglec-15-Fc and Siglec-15-His proteins in the supernatant was checked by Western blotting using anti-Fc antibody (Sigma-Aldorich) and anti-hexahistidine antibody (Qiagen), respectively. Siglec-15-Fc in the supernatant was purified with a HiTrap Protein A column (GE Healthcare UK) and the purity of the protein was confirmed as a single 56.4-kDa protein band by SDS-PAGE and silver staining. Siglec-15-His in the supernatant was purified with a HisTrap HP column, followed by Resource Q column chromatography (all from GE Healthcare UK), and a protein fraction which was not absorbed onto the column was collected as the purified protein fraction. The purity of the protein was confirmed as a single 31-kDa protein band by silver staining. Soluble forms of human Siglec-15 were generated in the same way that the soluble forms of

mouse Siglec-15 were produced. To amplify the extracellular domain of human Siglec-15 (amino acids 1-260), PCR was performed with the following two primers: 5'-ggggacaagttgtacaaaaagcaggcttcaccATGGAAAAGTCCATCTGGCTGC-3' and 5'-ggggaccactttgtacaagaaagctgggtcCCCGCTGGCGCCATGGAAGCGG-3'.

Anti-Siglec-15 polyclonal antibody

Rabbits were immunized by subcutaneous injection of a mixture of either mouse or human Siglec-15-Fc (100 or 50 µg, respectively) and oil adjuvant. The antiserum was applied to a HiTrap Protein A column to collect IgG proteins. Reactivity of the purified polyclonal antibody to Siglec-15 was confirmed by Western blotting analysis using both Siglec-15-Fc and Siglec-15-His proteins. Pre-immune rabbit IgG was purified from the serum, which was collected before immunization, with the same procedure as described above. The antibodies were further purified by affinity chromatography using the NHS-activated HiTrap column (GE Healthcare UK) immobilized with mouse or human Siglec-15-Fc.

In vitro osteoclast formation assay

Mouse BMM in the 96-well plate was cultured in the presence of 10 ng/mL M-CSF with 20 ng/mL RANKL or 30 ng/mL human tumor necrosis factor- α (TNF- α) (R&D Systems) for 3 days. Mouse UBMC was seeded at 5×10^5 cells/well in 96-well plates, and cultured in the presence of 2×10^{-8} M active vitamin D₃ or 80 ng/mL RANKL for 8 or 6 days, respectively. RAW264.7 cells were seeded at 4.5×10^3 cells/well in 96-well plates, and cultured in the presence of 40 ng/mL RANKL for 3 days. Human OCP was

seeded at 1×10^4 cells/well in 96-well plates, and cultured in the presence of 33 ng/mL M-CSF and 69 ng/mL RANKL for 5 days. During cultivation, cells were treated with anti-mouse or human Siglec-15 polyclonal antibody or pre-immune IgG. In the neutralization study, cells were treated with antigen-absorbed antibodies. Anti-mouse Siglec-15 polyclonal antibody was incubated with 1-, 3- and 10-fold higher concentrations of mouse Siglec-15-Fc or Siglec-15-His protein in Dulbecco's modified phosphate buffered saline containing 0.01% Tween 20 at 37°C for 2 h. After centrifugation, the supernatant of the mixture was collected as an antigen-absorbed antibody. TRAP activity assay and TRAP staining were employed to determine the effect on osteoclast formation. For the TRAP activity assay, cells were fixed with 10% formaldehyde, and incubated in a 0.1 M acetate buffer (pH 5.0) containing 50 mM sodium tartrate and 15 mM *p*-nitrophenyl phosphate as a substrate (all from Wako Pure Chemical Industries) for 10–30 min at room temperature. The reaction was stopped by adding 1 N NaOH, and an absorbance at 405 nm was measured to determine the amount of *p*-nitrophenol as catabolite. TRAP staining was performed by incubating the fixed cells in 0.1 M acetate buffer (pH 5.0) containing 50 mM sodium tartrate, 1% dimethylformamide (Wako Pure Chemical Industries), 0.27 mM naphthol AS-MX phosphate (Sigma-Aldorich) as a substrate and 1.6 mM Fast red violet LB salt (Sigma-Aldorich) as a stain for the reaction product for 5 min at room temperature. In the experiment using human OCP, TRAP-positive cells containing five or more nuclei were counted as multinuclear cells.

Statistical analysis

Welch's t test and Wilcoxon's rank sum test were used to identify GCT-related genes in *in silico* screening. A parametric Dunnett's test was used to examine the differences in osteoclast formation assays. A probability (*p*-value) of < 0.05 was considered significant.

Results

Identification of genes specifically up- or down-regulated in GCT

To identify GCT-related genes, I relied on the BioExpress System developed by Gene Logic, containing Affymetrix U133 oligonucleotide microarray expression profiles of numerous human samples from normal and diseased tissue types. The expression level of 10,259 probe sets was found to be significantly up- or down-regulated in GCT samples compared with those in normal and other tumor samples. To exclude genes which have less relationship with osteoclastogenesis, the probe sets were further examined to see if their expression pattern correlated with that of RANK and RANKL, both of which are known as key regulatory molecules in osteoclastogenesis [14-16]. The screening identified 709 probe sets whose expression levels were positively or negatively correlated with RANK or RANKL. These probe sets represented a set of genes that included known osteoclast marker genes, such as cathepsin K or TRAP (Table 1). Next, I utilized the TMHMM program in order to identify suitable drug targets from the selected 709 probe sets based on their predicted topology. CD84, Siglec-15, MEGF10 and CLEC4A were predicted to possess one transmembrane domain and considered as possible drug targets. In addition, the expression levels of these four genes were markedly up-regulated in GCT and highly correlated with those of RANK or RANKL (Table 1). I hypothesized that these genes were involved in osteoclastogenesis, and selected them as genes to be further examined.

Expression of Siglec-15 and other GCT-related genes in osteoclasts

To examine the expression profiles of the selected four GCT-related genes in normal

osteoclastogenesis, I analyzed mRNA expression levels in osteoclasts prepared from mouse macrophage RAW264.7 cells treated with RANKL [38], and mouse UBMC treated with active vitamin D₃ [39] (Table 2). The relative mRNA expression of CD84 slightly increased (1.9-fold) by active vitamin D₃ treatment in UBMC, while remained unchanged in RANKL-treated RAW264.7 cells. MEGF10 was not detected in either RAW264.7 cells or UBMC. CLEC4A expression remained unchanged or even decreased in osteoclasts differentiated from these cells. In contrast to these genes, the mRNA expression of Siglec-15 markedly increased in both RANKL-treated RAW264.7 cells (13.8-fold) and active vitamin D₃-treated UBMC (6.3-fold) compared with respective untreated cells. These results led me to speculate that Siglec-15 is the most probable gene involved in osteoclastogenesis, and to prioritize this gene for further examinations.

Next, I analyzed mRNA expression of Siglec-15 and a couple of osteoclast-specific genes, such as cathepsin K and TRAP in the course of osteoclast differentiation using RAW264.7 cells (Fig. 2). The expression of mRNA for Siglec-15 increased in a time-dependent manner from 2 days after RANKL stimulation. This expression pattern was closely related to those of osteoclast-specific genes, particularly to cathepsin K. The expression profile of Siglec-15 was further analyzed in a human osteoclast culture prepared from commercially available human OCP (Fig. 2). In a similar fashion to cathepsin K and TRAP, Siglec-15 expression was markedly up-regulated by RANKL stimulation in the cells.

Inhibitory effect of anti-Siglec-15 polyclonal antibody on osteoclast formation

To examine the functional role of Siglec-15 in osteoclast differentiation, I developed polyclonal antibodies for both mouse and human Siglec-15 and tested the effects of the antibodies in a variety of osteoclast culture systems. In primary mouse BMM culture system, which does not contain any adherent bone marrow cells such as stromal cells, anti-mouse Siglec-15 antibody decreased TRAP activity in cells stimulated with RANKL or TNF- α (Fig. 3A) in a concentration-dependent manner. The antibody also inhibited the increase in TRAP activity in a primary culture of mouse UBMC, which contains stromal or osteoblastic cells induced by active vitamin D₃ treatment (Fig. 3A). These inhibitory effects on TRAP activity were not observed when the cells were treated with purified pre-immune IgG. TRAP staining demonstrated that anti-Siglec-15 antibody treatment markedly inhibited RANKL-induced osteoclast differentiation from mouse UBMC to TRAP-positive multinuclear osteoclasts in comparison with pre-immune IgG-treated cells (Figs. 3B).

To confirm that the inhibitory effect of the antibody is mediated by Siglec-15 recognition, anti-mouse Siglec-15 polyclonal antibody was absorbed with mouse Siglec-15 proteins conjugated with human Fc or hexahistidine tag and tested in mouse osteoclast culture systems. In mouse BMM culture, the inhibitory effect of anti-Siglec-15 antibody on TRAP activity was neutralized by absorption with its antigen (Fig. 3C). A similar result was obtained when RAW264.7 cells were treated with antigen-absorbed antibody (Fig. 3D). These results suggest that the inhibitory activity of the antibody on osteoclast formation is mediated by specific binding of the antibody to Siglec-15 protein expressed on the cells.

Finally, I examined the effect of anti-human Siglec-15 polyclonal antibody on osteoclast formation from human OCP (Fig. 4). TRAP staining demonstrated that treatment with anti-Siglec-15 antibody inhibited multinuclear cell formation induced by RANKL in comparison with control or pre-immune IgG-treated cells. Quantitative analysis showed that the number of TRAP-positive multinuclear osteoclasts significantly decreased with anti-Siglec-15 antibody treatment.

Table 1

Gene expression analysis in GCT.

Gene name	Affymetrix ID	Gene expression (Intensity)		Pearson correlation	
		GCT	Normal/Other	RANK	RANKL
RANK	207037_at	138 ± 37	16 ± 14	1.00	0.75
RANKL	210643_at	194 ± 153	27 ± 23	0.75	1.00
Cathepsin K	202450_s_at	8260 ± 3284	1843 ± 1379	0.81	0.84
TRAP	204638_at	4600 ± 1099	507 ± 639	0.88	0.88
CD84	205988_at	571 ± 272	128 ± 74	0.89	0.72
Siglec-15	215856_at	623 ± 230	62 ± 38	0.84	0.73
MEGF10	232523_at	1623 ± 1072	200 ± 169	0.71	0.79
CLEC4A	219947_at	522 ± 200	62 ± 37	0.90	0.80

The expression levels of indicated genes in GCT were compared with those in normal and other tumor samples using the BioExpress database. The genes were further analyzed regarding Pearson's correlation with RANK and RANKL in their expression levels using in-house Perl programs. Gene expression data is expressed as the mean ± standard deviation ($n = 12-17$).

Table 2

Relative mRNA expression levels of GCT-related genes in mouse osteoclasts.

Gene name	RAW264.7		UBMC	
	Control	RANKL	Control	VD ₃
CD84	0.0070	0.0075	0.17	0.33
Siglec-15	0.0016	0.022	0.0015	0.0094
MEGF10	ND	ND	ND	ND
CLEC4A	0.042	0.028	0.026	0.022

Expression of mRNA was analyzed by real-time RT-PCR using mRNA for ribosomal protein L32 as an endogenous control. RAW264.7 was treated with or without 40 ng/mL RANKL for 3 days. UBMC was treated with or without 2×10^{-8} M active vitamin D₃ for 8 days. Data represents the value from one sample. ND: not detected.

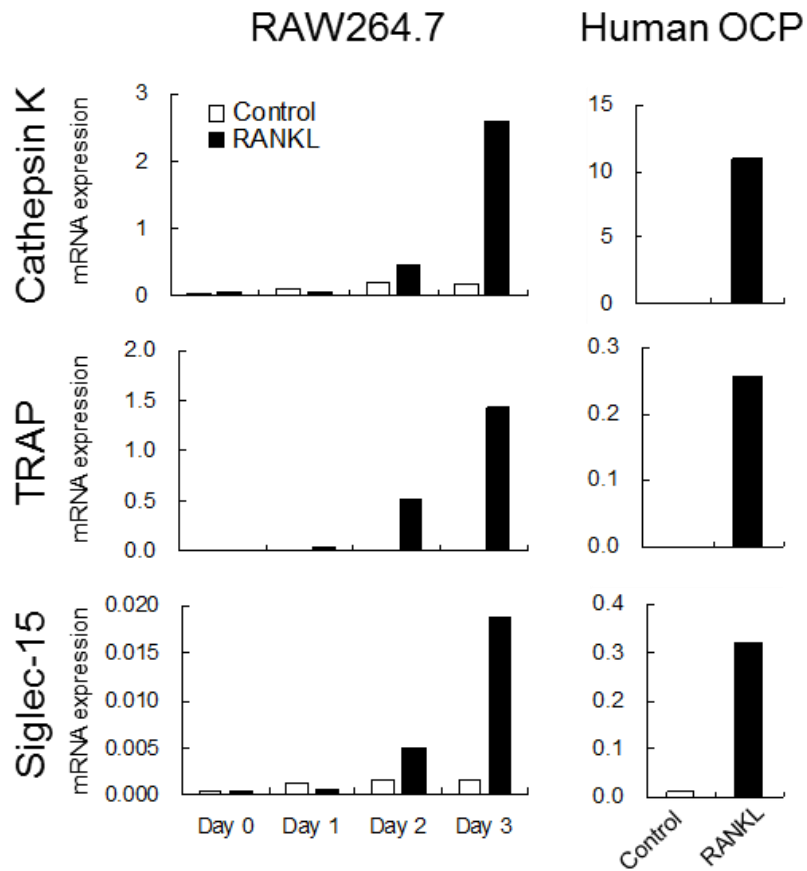


Fig. 2. Siglec-15 mRNA expression during osteoclast differentiation. Expression of mRNA for cathepsin K, TRAP or Siglec-15 was analyzed by real-time RT-PCR using mRNA for ribosomal protein L32 as an endogenous control. Total RNA was extracted from RAW264.7 treated with or without 40 ng/mL RANKL for the indicated periods. Total RNA was extracted from human OCP treated with either 33 ng/mL M-CSF alone or in combination with 53.2 ng/mL RANKL for 3 days. Data represents the value from one sample.

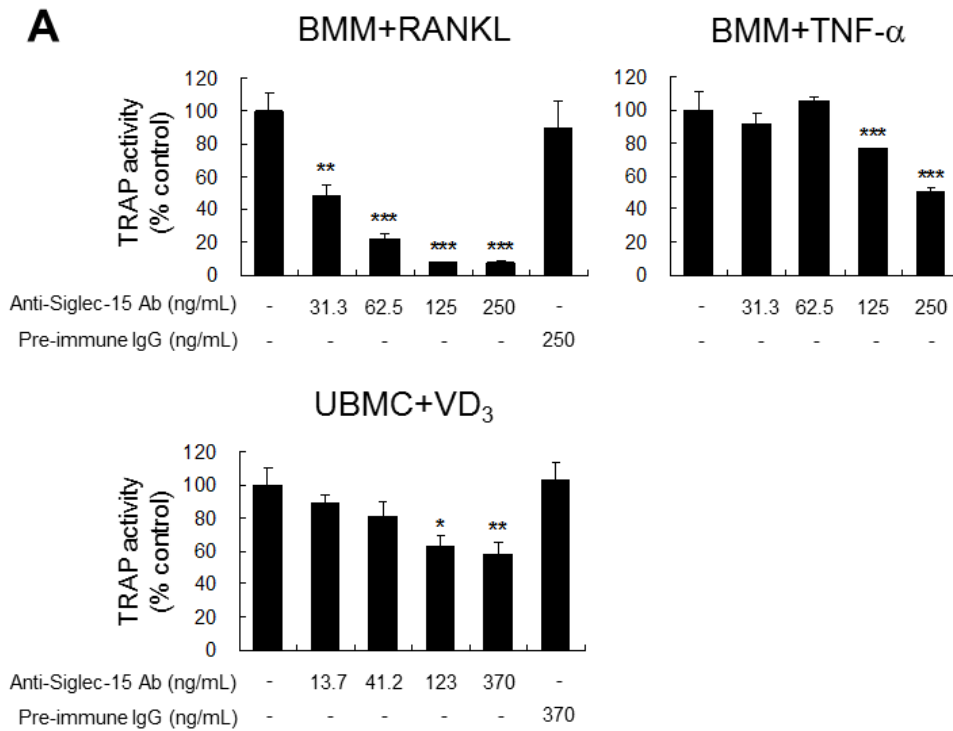
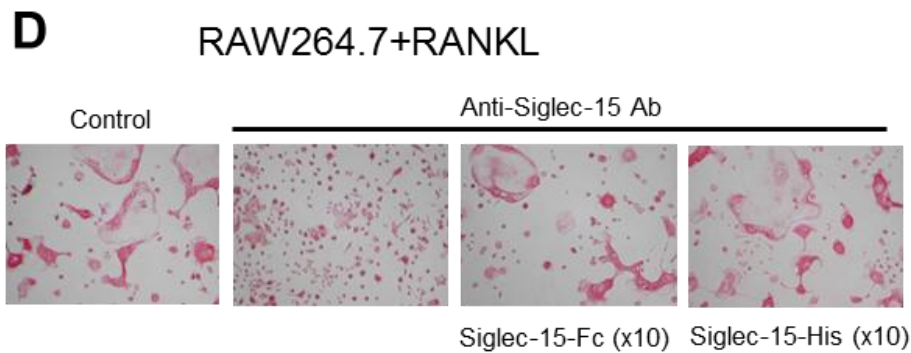
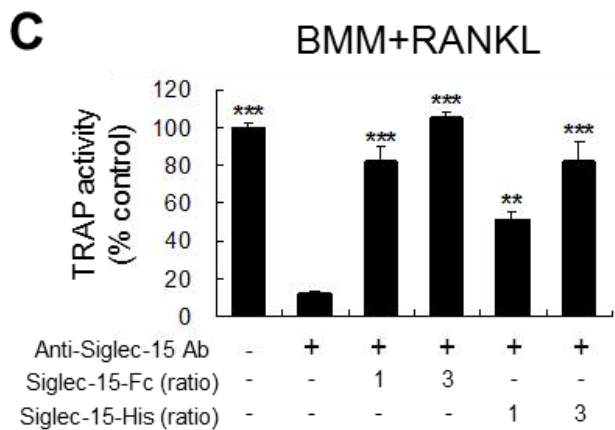


Fig. 3A. Effect of anti-Siglec-15 antibody (Ab) on mouse osteoclast formation. Mouse BMM was treated with the indicated concentrations of anti-mouse Siglec-15 Ab or pre-immune IgG in the presence of 10 ng/mL M-CSF and either 20 ng/mL RANKL or 30 ng/mL TNF- α for 3 days. Mouse UBMC was treated with antibodies in the presence of 2×10^{-8} M active vitamin D₃ for 8 days. TRAP activity of the cells was measured as an indicator for osteoclast differentiation. Data represents the mean \pm standard error ($n = 3-6$). * $p < 0.05$, ** $p < 0.01$ and *** $p < 0.001$ compared with no treatment control cells.



Fig. 3B. Effect of anti-Siglec-15 antibody (Ab) on mouse osteoclast formation. TRAP staining was performed to determine the effect on osteoclast formation. Mouse UBMC was treated with 3.3 $\mu\text{g}/\text{mL}$ anti-mouse Siglec-15 Ab or pre-immune IgG in the presence of 80 ng/mL RANKL for 6 days.



Figs. 3C and 3D. Neutralization of the effect of anti-Siglec-15 antibody (Ab) by its antigen. (C) Mouse BMM was treated with anti-mouse Siglec-15 Ab (0.5 $\mu\text{g}/\text{mL}$) absorbed or non-absorbed with its antigen in the presence of 10 ng/mL M-CSF and 20 ng/mL RANKL for 3 days. TRAP activity of the cells was measured as an indicator for osteoclast differentiation. Data represents the mean \pm standard error ($n = 3$). $**p < 0.01$ and $***p < 0.001$ compared with non-absorbed Ab-treated wells. (D) RAW264.7 cells were treated with anti-mouse Siglec-15 Ab (1 $\mu\text{g}/\text{mL}$) absorbed or non-absorbed with its antigen in the presence of 40 ng/mL RANKL for 3 days, and stained for TRAP activity.

Human OCP+RANKL

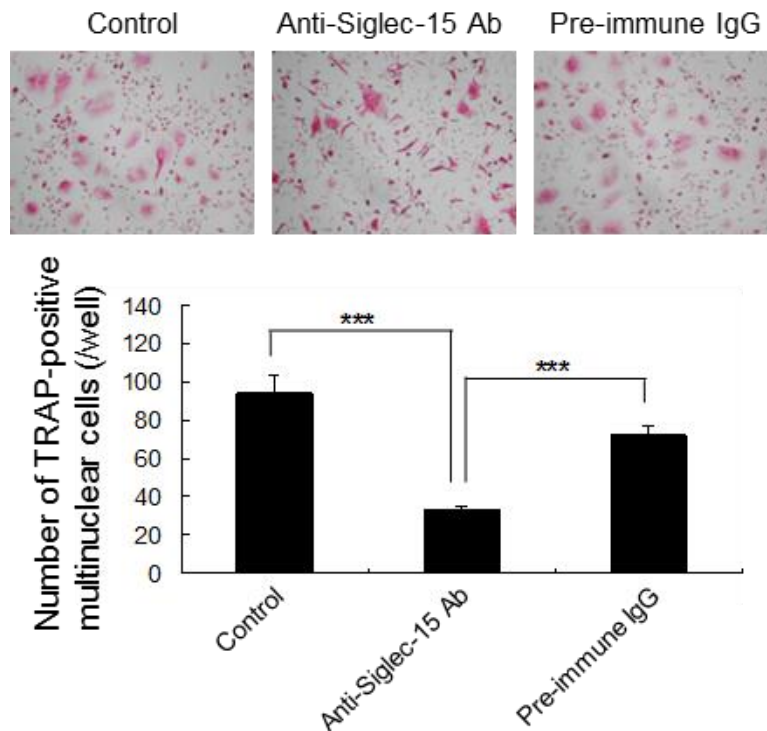


Fig. 4. Effect of anti-Siglec-15 antibody (Ab) on human osteoclast formation. Human OCP was treated with 30 $\mu\text{g}/\text{mL}$ anti-human Siglec-15 Ab or pre-immune IgG in the presence of 33 ng/mL M-CSF and 69 ng/mL RANKL for 5 days. TRAP staining was performed to determine the effect on osteoclast formation. TRAP-positive multinuclear cells containing more than 5 nuclei were counted as mature osteoclasts. Data represents the mean \pm standard error ($n = 6$). *** $p < 0.001$ compared with anti-Siglec-15 Ab-treated wells.

Discussion

In order to discover novel drug target genes for metabolic bone diseases, I constructed a list of genes that were specifically up- or down-regulated in GCT utilizing the latest knowledge of bioinformatics. I thought that this was a rational approach since numerous osteoclast-like giant cells appear and severe resorptive bone destruction occurs in GCT [26]. Indeed, a number of osteoclast-related genes, such as cathepsin K and TRAP were included in the GCT-related gene list (Table 1). This confirmed the reliability of the list and I expected that the list contained some undiscovered osteoclast-related genes. I selected four candidates (CD84, Siglec-15, MEGF10 and CLEC4A) that were predicted to possess a single transmembrane domain from the GCT-related gene list. This kind of transmembrane protein is considered to be one of the potential druggable targets, and is relatively easy to analyze for its functionality by producing and using its recombinant soluble protein. Among the four selected candidates, only Siglec-15 gene expression was found to be up-regulated during normal osteoclast differentiation (Table 2). Although CD84 and MEGF10 have been reported to be overexpressed in GCT by other group as well [36], no clear correlation with osteoclast differentiation was observed in the present study. Though functional analysis would be required to elucidate their roles in osteoclastogenesis, these genes might be involved in tumorigenesis or expressed in cells other than those of an osteoclast-lineage in GCT.

Functional analysis using purified polyclonal antibody revealed that Siglec-15 is involved in both mouse and human osteoclastogenesis *in vitro*. In mouse culture systems, the extent of the inhibitory effect on TRAP activity varied in the culture

systems used. For example, anti-Siglec-15 antibody strongly inhibited the increase in TRAP activity in mouse BMM stimulated with RANKL, while moderate or partial inhibition was observed in BMM stimulated with TNF- α or in UBMC stimulated with active vitamin D₃ (Fig. 3A). In contrast, anti-Siglec-15 antibody strongly inhibited TRAP-positive multinuclear cell formation in mouse UBMC, RAW264.7 and human OCP culture systems (Figs. 3B, 3D and 4). These results suggest that Siglec-15 may play a role mainly in osteoclast cell fusion, the terminal process in osteoclast differentiation. This hypothesis may be supported by the observation that Siglec-15 expression pattern was closely related to that of cathepsin K, which is known as a late differentiation marker during osteoclastogenesis (Fig. 2).

In a recent publication, Takahata et al. reported that sialylation of cell surface glycoconjugates was required for proper osteoclast differentiation, especially for the cell fusion of osteoclast precursors [40]. As Siglec-15 was reported to recognize sialylated ligands [29], a direct functional link may be created between sialic acid recognition and the increasing expression of Siglec-15 in the differentiating osteoclasts, which may be required for proper osteoclastic cell fusion. It is also interesting to take into consideration that Siglec-15 associates with the activating adaptor molecule DNAX activation protein 12 (DAP12) [29], since DAP12 has been revealed to be critically involved in osteoclastogenesis as one of the key mediators of intracellular signals [18, 20].

In this study, I identified Siglec-15 as a gene overexpressed in both GCT and normal osteoclasts. Functional analysis using polyclonal antibody suggested that Siglec-15 plays an important role in osteoclast differentiation. These findings will provide new

opportunities for developing therapeutics targeting Siglec-15, such as antibody medication for the treatment of metabolic bone diseases.

Chapter 2
Impaired Osteoclast Differentiation and Function and Mild
Osteopetrosis Development in Siglec-15-deficient Mice

Summary

Sialic acid-binding immunoglobulin-like lectin 15 (Siglec-15) is a cell surface receptor for sialylated glycan ligands. In Chapter 1, I identified the upregulated *Siglec15* expression in differentiated osteoclasts and inhibition of osteoclast differentiation by anti-Siglec-15 polyclonal antibody, demonstrating Siglec-15 involvement in osteoclastogenesis *in vitro*. To discern the physiological role of Siglec-15 in skeletal development and osteoclast formation and/or function *in vivo*, I generated Siglec-15-deficient (*Siglec15^{-/-}*) mice and analyzed their phenotype. The *Siglec15^{-/-}* mice developed without physical abnormalities other than increased trabecular bone mass in lumbar vertebrae and metaphyseal regions of the femur and tibia, causing mild osteopetrosis. Histological analyses demonstrated that the number of osteoclasts present on the femoral trabecular bone of the mutant mice was comparable to that of the wild-type mice. However, urinary deoxypyridinoline, a systemic bone resorption marker, decreased in the *Siglec15^{-/-}* mice, indicating that impaired osteoclast function was responsible for increased bone mass in the mutant mice. In addition, the ability of bone marrow-derived monocyte/macrophage cells from the *Siglec15^{-/-}* mice to differentiate into osteoclasts was impaired, as determined *in vitro* by cellular tartrate-resistant acid phosphatase activity in response to the receptor activator of nuclear factor- κ B ligand or tumor necrosis factor- α . These results reveal the importance of Siglec-15 in the regulation of osteoclast formation and/or function *in vivo*, providing new insights into osteoclast biology.

Introduction

Development and maintenance of the skeletal system depends on the balance between bone formation by osteoblasts and bone resorption by osteoclasts, and these opposing processes interact, forming a functional coupling [2, 41]. Osteoblasts, derived from mesenchymal stem cells, exist on the bone surface and synthesize bone matrix. In functional coupling, osteoblasts regulate osteoclast formation both by secreting factors, including macrophage colony-stimulating factor (M-CSF), interleukin-1 (IL-1), and IL-6 [11], and by direct interaction with osteoclast precursors [12, 13]. Conversely, osteoclasts are multinucleated cells positive for tartrate-resistant acid phosphatase (TRAP) generated from mononuclear monocyte/macrophage lineage hematopoietic precursors [10], which resorb bone by secreting protons and proteases into resorption zones. Accordingly, mice carrying mutated genes responsible for osteoclast formation and/or function exhibit increased bone mass (osteopetrotic phenotype) caused by impaired bone resorption [42, 43]. During osteoclastogenesis, the receptor activator of nuclear factor- κ B ligand (RANKL)—produced by cells of osteoblastic lineage—binds to its receptor, receptor activator of nuclear factor- κ B (RANK)—expressed on the cell surface of osteoclast precursors—triggering key intracellular signaling cascades [15, 16, 44].

Together with RANK/RANKL signaling, costimulatory signals mediated by immunoreceptor tyrosine-based activation motif (ITAM)-bearing adaptor proteins are required for the terminal differentiation of osteoclasts [18-20]. DNAX-activating protein of 12 kDa (DAP12) is one such ITAM-bearing adaptor; its deficiency is reportedly associated with skeletal abnormalities in mice and humans, suggesting the involvement

of this signaling pathway in regulating osteoclast development and/or function [21-25]. ITAM-bearing adaptor proteins have minimal extracellular binding domains and are thought to convey extracellular signals through interaction with ligand-binding, immunoglobulin-like receptors (IgLRs). Triggering receptor expressed on myeloid cells 2 (TREM-2), signal-regulatory protein β 1, and myeloid DAP12-associating lectin-1 are IgLRs expressed on osteoclasts, and candidate DAP12-associating partners [18, 20, 25]. However, studies in mutant mice have not yet clarified the relevance of these genes in bone homeostasis, implying the existence of undiscovered DAP12-associated receptors critical for osteoclastogenesis.

Sialic acid-binding immunoglobulin-like lectin 15 (Siglec-15) is a newly identified member of the Siglec family of cell-surface IgLRs that recognizes sialylated glycan ligands [27-29]. Siglec-15 reportedly associates more avidly with DAP12 than other ITAM-bearing signaling adaptors, such as the DNAX-activating protein of 10 kDa or Fc receptor γ subunit (FcR γ), in 293T cells co-transfected with constructs expressing these genes [29]. Although a certain regulatory role in the immune system has been suggested based on its gene expression in macrophages and/or dendritic cells [29], the physiological role of Siglec-15 in vertebrates remains unknown. In Chapter 1, I demonstrated that *Siglec15* expression was upregulated during osteoclast differentiation in mouse and human osteoclast culture systems. Moreover, functional analysis using a polyclonal antibody against Siglec-15, demonstrated an inhibitory effect on osteoclast formation *in vitro*, suggesting that Siglec-15 is critical to osteoclastogenesis. To elucidate the physiological role of this gene *in vivo*, especially during osteoclastogenesis and skeletal development, I generated Siglec-15-deficient (*Siglec15*^{-/-}) mice and

analyzed their phenotype.

Materials and Methods

Gene targeting and generation of Siglec15^{-/-} mice

Genomic clones encoding the *Siglec15* locus were isolated from a 129S6/SvEvTac mouse bacterial artificial chromosome library by screening with a radiolabeled DNA fragment of a 550-base pair region of exon 1. A targeting vector was constructed by replacing exons 2–4, encoding two immunoglobulin-like domains and a transmembrane domain, with a phosphoglycerate kinase neomycin resistance cassette. The linearized targeting vector was electroporated into 129 Sv/EvTac-derived embryonic stem cells. G418-resistant colonies were genotyped by PCR and genomic Southern blot analyses to identify clones carrying a targeted allele. Targeted cells were injected into C57BL/6 blastocysts, and transferred into pseudopregnant female ICR mice. Resulting chimeric males were bred with C57BL/6 females; heterozygous offspring were then backcrossed to the C57BL/6 strain for 7–8 generations by *in vitro* fertilization. Following heterozygous matings of backcrossed animals, the *Siglec15^{-/-}* mice were identified by Southern blot analysis of genomic DNA cut with *KpnI* using a specific probe. All procedures described here were performed at PhoenixBio Co., Ltd.

Animal experiments

Experimental procedures were performed in accordance with the in-house guidelines of the Institutional Animal Care and Use Committee of Daiichi Sankyo Co., Ltd. Seven-week-old male and female *Siglec15^{-/-}* mice and their wild-type littermates were obtained from PhoenixBio Co., Ltd. The animals were fed a normal diet and given tap water *ad libitum* under a controlled room temperature and humidity. Whole-body

microradiographs were performed using a μ FX-1000 radiography system (Fujifilm) and BAS-2500 imaging system (Fujifilm) on anesthetized mice 4 days before necropsy. Body weight was measured 1 day before necropsy.

At 18 weeks of age, the mice were euthanized by exsanguination after collecting blood samples from the inferior vena cava under anesthesia. Whole blood samples were used for hematological and blood chemical analyses. Lumbar vertebrae, femurs, and tibiae were excised for bone phenotypic analysis. Thoracic and abdominal organs were observed macroscopically, and the liver, thymus, spleen, and testes were weighed. The following organs/tissues were histopathologically examined: sternum (bone marrow), thymus, lung, heart, mesenteric lymph node, liver, spleen, kidney, adrenal gland, pancreas, stomach, duodenum, jejunum, ileum, cecum, colon, rectum, thyroid (including parathyroid), testis (male), ovary (female), uterus (female), tibia (bone marrow), eye, and skin (dorsal region). Testes were fixed with FSA, eyes with Davidson's fixative, and other organs/tissues with 10% neutral-buffered formalin. After fixation, histopathological sections were prepared and stained with hematoxylin and eosin.

Bone densitometry and micro-CT imaging

After removing connective tissue, excised lumbar vertebrae (L3–6) and paired femurs were defatted and dehydrated by ethanol treatment, with subsequent air seasoning.

Areal bone mineral density of the lumbar vertebrae and femurs was measured by dual-energy X-ray absorptiometry using a DCS-600EX-IIIIR (Aloka) optimized for small bone specimens. The scan speed was 25 mm/s, and scan width was 1 mm. Bone

mineral density analysis was performed based on single energy (22 keV) X-ray absorption data for lumbar vertebrae L3–6 and 20 equally divided femoral regions.

Right femoral volumetric bone mineral content (vBMC) was measured by peripheral quantitative computed tomography (pQCT) using XCT Research SA+ (Stratec Medizintechnik) and XCT6.20 analyzing software (Stratec Medizintechnik) at ELK Corporation. Two slices were measured with an $80 \times 80 \times 460 \mu\text{m}$ voxel size at 2 mm proximal to the distal femoral growth cartilage for trabecular regions and the femoral midpoint for cortical regions. Trabecular bone in the metaphysis and cortical bone in the diaphysis were analyzed with contour mode 2, with peel mode 20 (trabecular area 35%), and contour mode 1 using a threshold of 690 mg/cm^3 , respectively.

Micro-computed tomography (micro-CT) imaging of the fifth lumbar vertebra was performed using ScanXmate-L080H (Comscantecno), with a voxel size of $14 \mu\text{m}$ in three dimensions. Three-dimensional images were reconstructed using bone structural analysis software, TRI/3D-BON (RATOC System Engineering).

TRAP staining of bone

Right tibiae were excised and fixed in cold 70% ethanol. Processing of bone specimens was performed at Kureha Special Laboratory Co., Ltd. Proximal tibiae were dehydrated in graded ethanol concentrations and embedded in glycol methacrylate (Wako Pure Chemical Industries) without decalcification. Frontal plane sections ($3 \mu\text{m}$ thick) of the proximal metaphysis were prepared using an RM2255 rotary microtome (Leica Microsystems, Germany) and stained for TRAP activity using a method adapted from that previously described [45]. Hematoxylin and eosin staining was performed

using histopathological sections of tibiae fixed with 10% neutral-buffered formalin.

Bone histomorphometry

Mice were subcutaneously injected with calcein (20 mg/kg; Dojindo) and tetracycline hydrochloride (20 mg/kg; Sigma-Aldrich) 7 and 3 days prior to dissection, respectively. At necropsy, right femurs were excised and fixed in 70% ethanol, and adherent muscle was removed. Bone specimen processing and histomorphometry in cortical and cancellous bone were performed at Ito Bone Histomorphometry Institute. Distal and central femurs were stained with Villanueva bone stain for 5 days, dehydrated in graded ethanol concentrations, and embedded in methyl methacrylate (Wako Pure Chemical Industries) without decalcification. For cancellous bone histomorphometry, frontal plane sections (5 μm thick) of the distal metaphysis were prepared using the RM2255 rotary microtome. The region of interest was located 0.25 mm–1.00 mm proximal to the distal femoral growth cartilage/metaphyseal junction, and 0.25 mm from the endosteal border of the cortices. Measurements were collected at 400 \times magnification using the semiautomatic image analyzing system, Histometry RT (System Supply), linked to a BX-51 light/epifluorescent microscope (Olympus). The following parameters were measured: bone volume per total tissue volume, trabeculae number, and osteoblast surface, osteoclast surface, and bone formation rate per unit bone surface. Cortical bone histomorphometry was performed on femoral midpoint cross-sections ground to a 10- to 20- μm -thickness using a Speed Lap ML-521 (Maruto Instrument). Cortical area, osteoid surface, eroded surface, and labeled surface were measured per unit periosteal bone surface. Standard bone histomorphometric nomenclature, symbols, and units were used

according to the American Society of Bone and Mineral Research Histomorphometry Nomenclature Committee [46].

Measurement of bone metabolic markers

Urine samples were collected by gently pushing the abdomen of 9- and 18-week-old animals. Urinary deoxypyridinoline (DPD) excretion was measured using an enzyme-linked immunosorbent assay kit from DS Pharma Biomedical Co., Ltd. To compensate for individual variation in DPD excretion, urinary creatinine concentration was also measured using an assay kit (Kainos) according to the manufacturer's instructions. Serum samples prepared at necropsy were used to measure levels of the bone formation marker, osteocalcin (Mouse Osteocalcin EIA kit; Biomedical Technologies). A microplate reader, SpectraMax 250 (Molecular Devices), was used for each assay.

in vitro osteoclast formation assay

Mouse bone marrow-derived monocyte/macrophage (BMM) cells were prepared according to previously described methods, with slight modifications [18]. In brief, bone marrow cells were flushed from femurs and tibiae of the 10-week-old male *Siglec15^{-/-}* or wild-type mice, and seeded to flasks with α -MEM (Life Technologies), containing 5 ng/mL human M-CSF (R&D Systems), 10% fetal bovine serum, 100 μ g/mL streptomycin, and 100 U/mL penicillin. After being cultured overnight, nonadherent cells were collected and suspended at 1.5×10^5 cells/mL in medium containing 10 ng/mL human M-CSF alone for the RANKL-induced osteoclast

formation assay, or human M-CSF in combination with 2 ng/mL human transforming growth factor- β (R&D Systems) for the tumor necrosis factor- α (TNF- α)-induced assay. The cells were then seeded in 96-well plates (0.2 mL/well), and cultured for 2 days to generate mouse BMM. After replacing old medium with fresh medium, cells were cultured in medium containing 10 ng/mL M-CSF, and 30 ng/mL human RANKL (PeproTech) or 30 ng/mL human TNF- α (R&D Systems) for an additional 4 days. For the TRAP activity assay, cells were solubilized with 50 μ L of 50 mM sodium citrate buffer (pH 6.1) containing 1% Triton X-100, and incubated with 50 μ L of 50 mM sodium citrate buffer (pH 6.1), containing 5 mg/mL *p*-nitrophenyl phosphate (Sigma-Aldrich) and 0.46% sodium tartaric acid, for 20 min at room temperature. The reaction was stopped by adding 50 μ L of 1 N NaOH, and an absorbance at 405 nm was measured using a SpectraMax 250 to determine the amount of *p*-nitrophenol as a catabolite.

Statistical analysis

Mean and standard error were calculated using Excel 2003. All statistical analyses were conducted using an in-house program, based on SAS System, Release 8.2, SAS Institute. Comparison between the wild-type and *Siglec15*^{-/-} littermates was performed by the F-test of variance, followed by Student's *t*-test (homogeneous variance) or Welch's *t*-test (non-homogeneous variance). A *p* value of <0.05 was considered significant.

Results

Generation of Siglec15^{-/-} mice

To disrupt *Siglec-15* in mice, I designed a targeting vector to replace exons 2–4 with a neomycin resistance cassette (Figs. 5A, 5B), deleting most of the extracellular and transmembrane domains of the Siglec-15 protein. Southern blot analysis of 4-week-old offspring of heterozygous matings revealed that the *Siglec15^{-/-}* mice were born in approximately Mendelian ratios (+/+ : 149 [27%]; +/- : 280 [51%]; -/- : 118 [22%]). The *Siglec15^{-/-}* mice grew normally, without apparent physical abnormalities except for skeletal changes, according to body weight, hematology, blood chemistry, and pathological examinations performed on organs and tissues from 18-week-old mice, as described in the Materials and Methods. Although high *Siglec-15* mRNA expression was reported in the human spleen, testis, and small intestine [29], histopathological examinations detected no obvious abnormalities in these organs in the *Siglec15^{-/-}* mice.

Mild osteopetrotic phenotype in Siglec15^{-/-} mice

To analyze the phenotypic changes in skeletal tissues, I performed radiography and bone densitometry on 18-week-old *Siglec15^{-/-}* mice. Whole body radiography demonstrated that the skeletal phenotype in mutant mice resembled to that in the wild-type mice (Fig. 6A), without profound osteopetrotic hallmarks, such as long bone shortening or tooth eruption failure [47-49]. However, increased bone density was evident, especially in the distal femur and proximal tibia of the *Siglec15^{-/-}* mice (Fig. 6B). Measurement of areal bone mineral density confirmed this quantitatively, showing a marked increase, especially from the distal metaphysis to the midshaft of the

femur (Fig. 6C). In addition, pQCT demonstrated profoundly increased trabecular vBMC in the distal femoral metaphysis in the *Siglec15*^{-/-} mice (Fig. 6D). Increased vBMC was also observed in the cortical bone of the femoral diaphysis in the female mutant mice, although the increase was slight compared with that in trabecular bone. No vBMC increase was evident in the cortical bone of the male mutant mice, suggesting sexual dimorphism of the cortical bone phenotype. Next, I performed micro-CT imaging of lumbar vertebrae to observe the phenotype at sites other than long bones. Trabecular bone mass was markedly increased in the fifth lumbar vertebra of the *Siglec15*^{-/-} mice compared with the wild-type mice (Fig. 6E), consistent with areal bone mineral density of lumbar vertebrae L3–6 (Fig. 6F).

Histological and histomorphometrical analyses of the bone in Siglec15^{-/-} mice

I performed histological examinations on the hind limbs of the mutant mice to confirm an osteopetrotic phenotype and analyze morphological, quantitative, and dynamic changes in trabecular and cortical bone. Hematoxylin and eosin staining of longitudinal sections of the proximal metaphyseal tibia showed increased trabeculae number and trabecular bone volume, especially in the secondary spongiosa and epiphyseal ossification center, in the *Siglec15*^{-/-} mice (Fig. 7). No obvious histological changes were observed in the proximal tibial growth plate, consistent with the normal skeletal growth in the *Siglec15*^{-/-} mice (Fig. 6A). Despite increased bone mass, osteoclasts were detected by TRAP staining at primary and secondary spongiosa in the *Siglec15*^{-/-} mice, comparable to the wild-type mice (Fig. 7). In addition, bone histomorphometry of the distal femur demonstrated profound increases in both

trabecular bone volume per total tissue volume and trabeculae number, but no substantial changes in the percentage osteoclast surface per unit bone surface (Table 3). With regard to bone formation, osteoblast surface per unit bone surface and the bone formation rate per unit bone surface were markedly reduced in the *Siglec15^{-/-}* mice compared with the wild-type mice, suggesting that trabecular bone turnover was suppressed in the *Siglec15^{-/-}* mice. In cortical bone, the cortical area was slightly higher in the female mutant mice than in the wild-type mice, while no difference was evident in male mice, consistent with the pQCT-determined vBMC of the femoral diaphysis (Fig. 6D). In the female mutant mice, reduced eroded surface per unit periosteal bone surface and increased calcein- or tetracycline-labeled periosteal surface were evident, suggesting reduced bone resorption and enhanced bone formation. Conversely, in the male mutant mice, there were no clear changes in these parameters. Osteoid surface per unit periosteal bone surface did not change in the male or female mutant mice.

Changes in bone metabolic markers in Siglec15^{-/-} mice

To assess systemic bone turnover in the mutant mice, urinary DPD excretion and serum osteocalcin levels were measured as markers of bone resorption and formation, respectively. Urinary DPD excretion in both male and female mutant mice decreased compared with the wild-type mice at 9 and 18 weeks of age (Fig. 8A), indicating that overall bone resorption activity was reduced in the *Siglec15^{-/-}* mice. Conversely, at 18 weeks of age, osteocalcin levels were comparable in the male mutant mice and higher in the female mutant mice (Fig. 8B).

Impaired differentiation of Siglec15^{-/-} bone marrow-derived monocyte/macrophage cells into osteoclasts in vitro

I evaluated developmental differences in osteoclasts, induced *in vitro* from BMM of the wild-type and *Siglec15^{-/-}* mice by RANKL or TNF- α stimulation in the presence of M-CSF [18, 50]. Cellular TRAP activity, a marker of osteoclast differentiation, was upregulated in BMM from the wild-type mice by both RANKL and TNF- α treatment (Fig. 9). Although TRAP activity was upregulated in *Siglec15^{-/-}* BMM, it was lesser than that in the wild-type cells in both osteoclast formation culture systems. These results indicate that osteoclast differentiation is impaired, at least *in vitro*, by Siglec-15 deficiency.

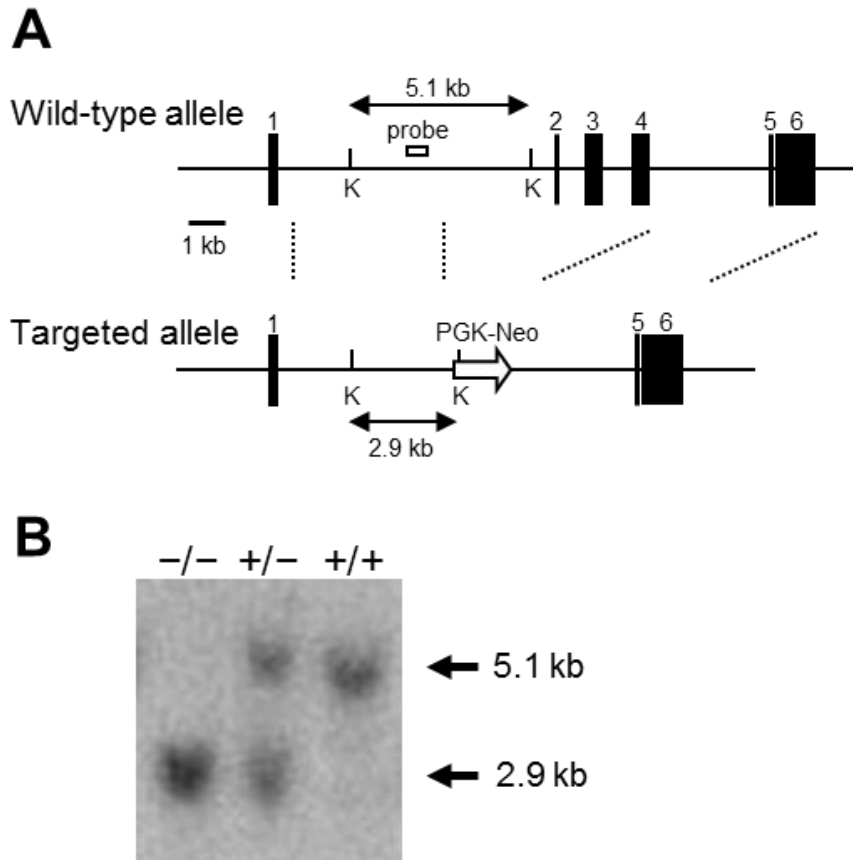
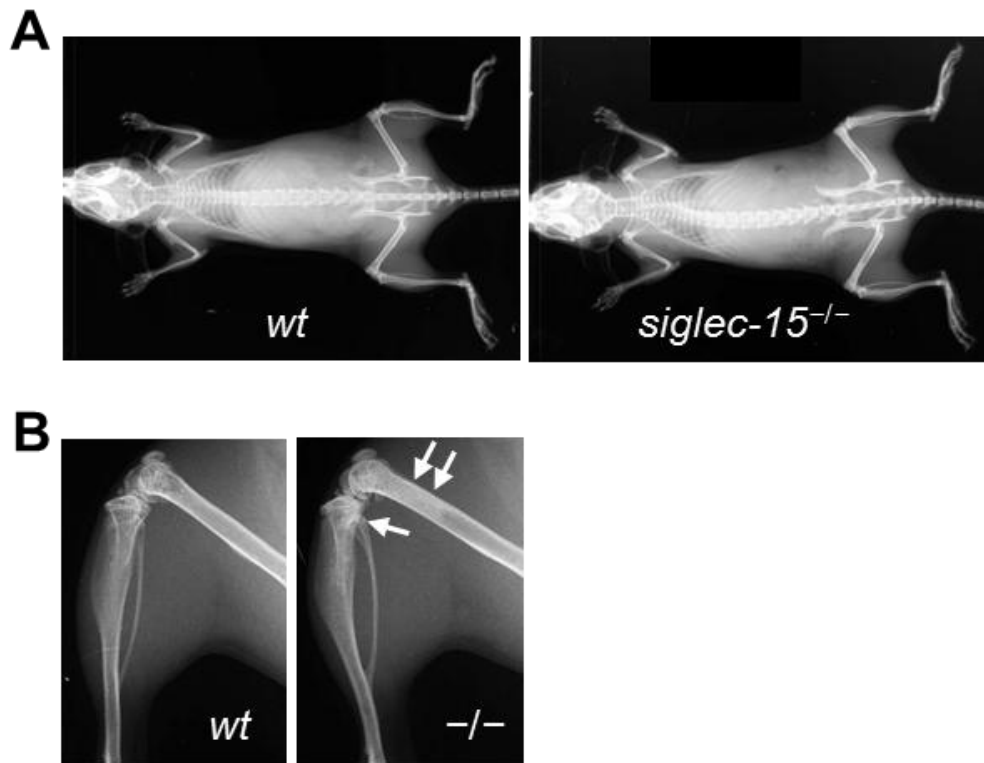
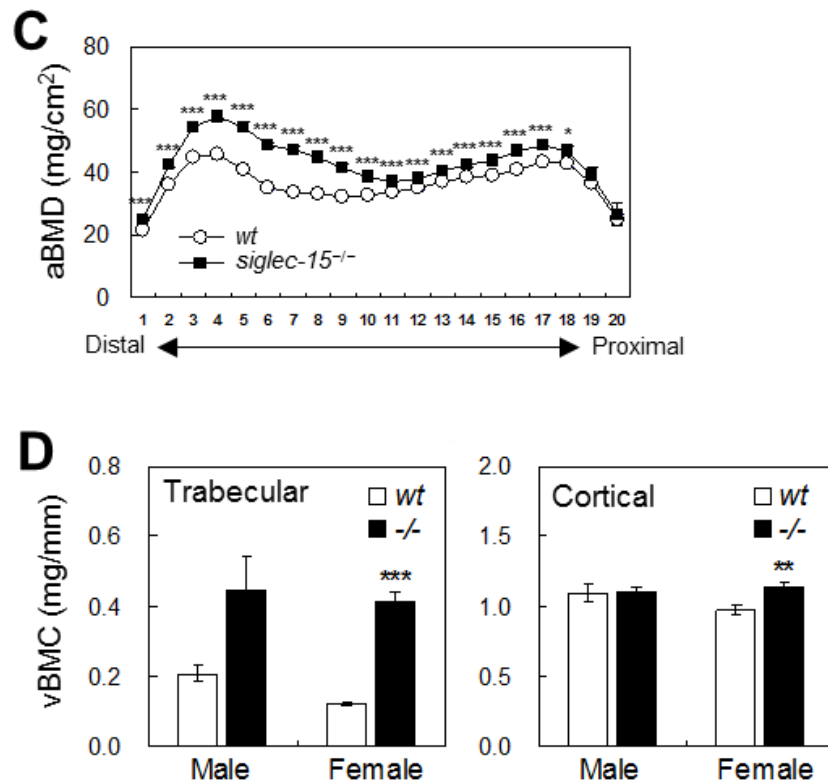


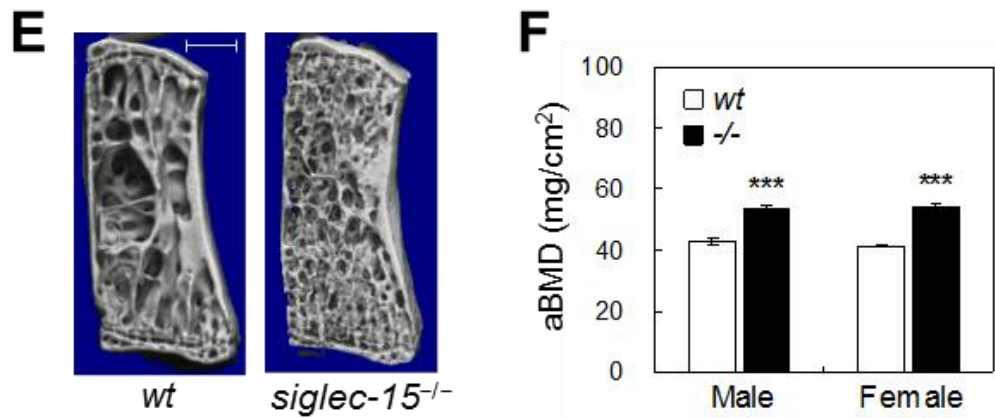
Fig. 5. Generation of *Siglec15*^{-/-} mice. (A) Schematic representation of the wild-type and targeted alleles at the *Siglec15* locus. Exons, represented by black boxes, are numbered. The phosphoglycerate kinase neomycin resistance cassette (PGK-neo) replaced the genomic region containing exons 2–4, encoding two immunoglobulin-like domains and a transmembrane domain of Siglec-15. An unfilled box indicates the probe for Southern blot analysis. K, *KpnI*. (B) Southern blot analysis of offspring derived from heterozygous matings. Genomic DNA from the wild-type (+/+), heterozygous (+/-), and homozygous (-/-) Siglec-15-deficient mice were digested with *KpnI* and hybridized with the probe. DNA fragments' sizes are indicated.



Figs. 6A and 6B. Representative radiographs of 18-week-old female wild-type and *Siglec15^{-/-}* mice. (A) Whole body radiographs and (B) magnified pictures of the left hind limb of the indicated mice. Arrows in the *Siglec15^{-/-}* mouse indicate increased radiodensity.



Figs. 6C and 6D. Increased bone mass in long bones in *Siglec15^{-/-}* mice. (C) Areal bone mineral density (aBMD) was measured in 20 longitudinal divisions of femurs from the female wild-type and *Siglec15^{-/-}* mice by dual-energy X-ray absorptiometry. (D) Volumetric bone mineral content (vBMC) of trabecular and cortical bone was analyzed by peripheral quantitative computed tomography at 2 mm proximal to the distal femoral growth cartilage and femoral midpoint, respectively. Data represent the mean \pm standard error from the 18-week-old male wild-type ($n = 10$), male *Siglec15^{-/-}* ($n = 7$), female wild-type ($n = 10$) or female *Siglec15^{-/-}* mice ($n = 9$). * $p < 0.05$, ** $p < 0.01$ and *** $p < 0.001$ compared with the wild-type mice of same sex.



Figs. 6E and 6F. Increment in bone volume at lumbar vertebrae of *Siglec15^{-/-}* mice. (E) Representative three-dimensional micro-computed tomography images of the fifth lumbar vertebrae of the 18-week-old female wild-type and *Siglec15^{-/-}* mice. Scale bar: 500 μ m. (F) aBMD was measured in the lumbar vertebrae L3–6 from the wild-type and *Siglec15^{-/-}* mice. Data represent the mean \pm standard error from the 18-week-old male wild-type ($n = 10$), male *Siglec15^{-/-}* ($n = 7$), female wild-type ($n = 10$) or female *Siglec15^{-/-}* mice ($n = 9$). *** $p < 0.001$ compared with the wild-type mice of same sex.

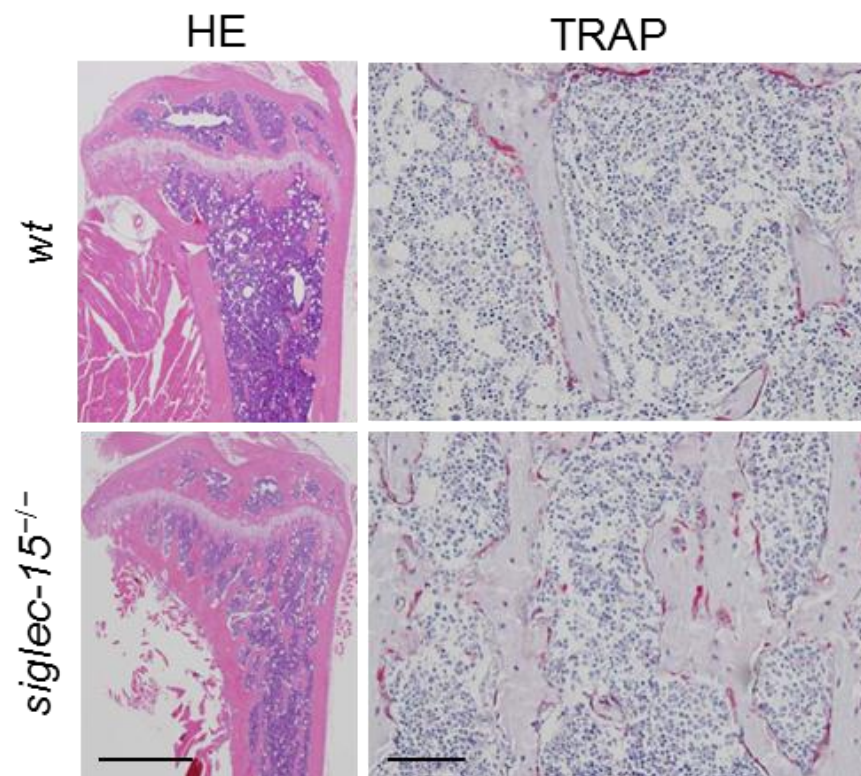


Fig. 7. Histologic evaluation of bone morphology in *Siglec15*^{-/-} mice. (*Left panels*) Hematoxylin and eosin staining of the proximal metaphysis of the right tibiae from the 18-week-old female wild-type and *Siglec15*^{-/-} mice. Scale bar: 1 mm. (*Right panels*) Magnified pictures of the primary spongiosa of proximal tibiae stained for TRAP activity to visualize osteoclasts in red. Scale bar: 100 μ m.

Table 3

Bone histomorphometrical analysis of femurs in wild-type and *Siglec15*^{-/-} mice.

Parameters	Wild-type	<i>Siglec15</i> ^{-/-}
Male		
Distal femoral metaphysis (cancellous bone)		
BV/TV (%)	9.66 ± 0.65	20.58 ± 2.19 ^b
Tb.N (#/mm)	3.49 ± 0.15	8.09 ± 0.97 ^b
Ob.S/BS (%)	19.18 ± 1.16	6.71 ± 1.05 ^c
Oc.S/BS (%)	7.702 ± 0.528	7.255 ± 0.860
BFR/BS (mm ³ /mm ² /y)	0.1492 ± 0.0100	0.0297 ± 0.0034 ^c
Femoral midshaft (cortical bone)		
Ct.Ar (mm ²)	0.8348 ± 0.0262	0.8537 ± 0.0101
Ps.OS/Ps.BS (%)	24.90 ± 2.60	25.65 ± 2.94
Ps.ES/Ps.BS (%)	14.98 ± 3.24	22.75 ± 3.09
Ps.LS/Ps.BS (%)	43.40 ± 1.83	37.99 ± 3.97
Female		
Distal femoral metaphysis (cancellous bone)		
BV/TV (%)	6.21 ± 0.60	24.62 ± 1.74 ^c
Tb.N (#/mm)	2.29 ± 0.17	7.71 ± 0.72 ^c
Ob.S/BS (%)	42.80 ± 2.52	13.34 ± 1.24 ^c
Oc.S/BS (%)	9.263 ± 1.002	8.646 ± 0.421
BFR/BS (mm ³ /mm ² /y)	0.3475 ± 0.0079	0.0776 ± 0.0094 ^c
Femoral midshaft (cortical bone)		
Ct.Ar (mm ²)	0.8326 ± 0.0145	0.9056 ± 0.0114 ^b
Ps.OS/Ps.BS (%)	37.03 ± 2.77	38.69 ± 3.71
Ps.ES/Ps.BS (%)	21.88 ± 2.66	7.58 ± 1.31 ^c
Ps.LS/Ps.BS (%)	46.82 ± 3.39	59.09 ± 3.36 ^a

BV/TV: bone volume/tissue volume; Tb.N: trabecular number; Ob.S/BS: osteoblast surface/bone surface; Oc.S/BS: osteoclast surface/bone surface; BFR/BS: bone formation rate/bone surface; Ct.Ar: cortical area; Ps.OS/Ps.BS: periosteal osteoid surface/bone surface; Ps.ES/Ps.BS: periosteal eroded surface/bone surface; Ps.LS/Ps.BS: labeled periosteal surface/bone surface. Data represent the mean ± standard error from 18-week-old male wild-type (n = 8), male *Siglec15*^{-/-} (n = 8), female wild-type (n = 6) or female *Siglec15*^{-/-} mice (n = 9). ^a*p* < 0.05, ^b*p* < 0.01, and ^c*p* < 0.001 compared with wild-type mice.

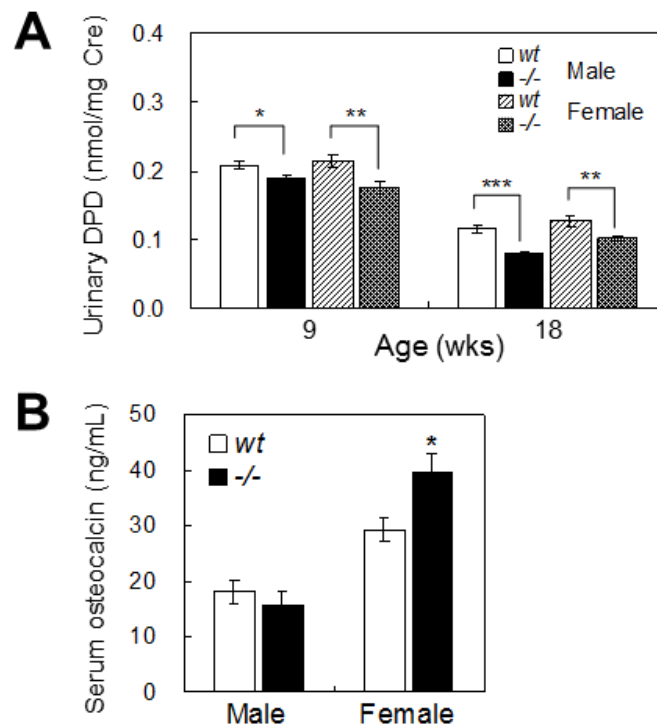


Fig. 8. Changes in bone turnover markers in *Siglec15*^{-/-} mice. (A) Urine samples were collected from the wild-type and *Siglec15*^{-/-} mice at 9 and 18 weeks of age. Urinary deoxypyridinoline (DPD) excretion was measured, and adjusted for creatinine (Cre) concentration. (B) Serum levels of osteocalcin were determined with samples prepared from the 18-week-old wild-type and *Siglec15*^{-/-} mice. Data represent the mean \pm standard error from the male wild-type (n = 10), male *Siglec15*^{-/-} (n = 7), female wild-type (n = 10), and female *Siglec15*^{-/-} mice (n = 9), with the exception of urinary DPD excretion at 9 weeks of age, where male wild-type (n = 9), and male *Siglec15*^{-/-} (n = 5). **p* < 0.05, ***p* < 0.01, and ****p* < 0.001 compared with the wild-type mice of the same sex.

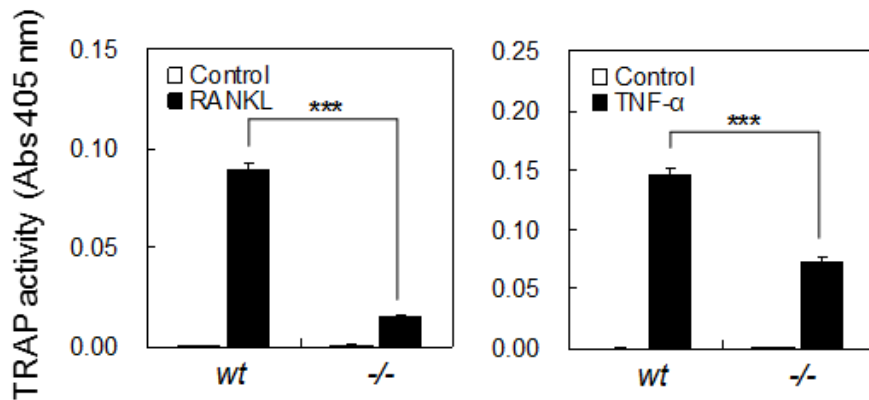


Fig. 9. Osteoclast formation assay using bone marrow-derived monocyte/macrophage cells derived from the wild-type and *Siglec15*^{-/-} mice. Bone marrow-derived monocyte/macrophage cells were prepared from the 10-week-old male wild-type and *Siglec15*^{-/-} mice. Cells were cultured with 30 ng/mL RANKL, or 30 ng/mL TNF- α , for 4 days in the presence of 10 ng/mL M-CSF. TRAP activity was measured as an indicator of osteoclast differentiation. Data represent the mean \pm standard error (n = 12) from one experiment. *** $p < 0.001$ compared with wild-type cells.

Discussion

Osteopetrosis is a heterogeneous group of heritable genetic diseases, characterized by increased bone mass due to defective osteoclastic bone resorption [42, 43]. In mice, many genes associated with increased bone mass have been identified by mutant studies, revealing that osteopetrosis severity depends on genes functional in osteoclast differentiation and/or function. Osteopetrosis in the *Siglec15*^{-/-} mice was mild compared with, for example, c-Fos or RANK knockout mice, which exhibit a severe osteopetrotic phenotype, including long bone shortening and tooth eruption failure [47-49]. My observations suggest Siglec-15 deficiency causes partial reduction of bone resorption, leading to mild osteopetrosis *in vivo*. Reduced bone resorption was evident from lower urinary DPD excretion, while trabecular bone mass increased, despite comparable osteoclast numbers on femoral and tibial trabecular bone. These findings suggest that impaired osteoclast function, but not reduced osteoclast number, underlies the osteopetrotic phenotype of the *Siglec15*^{-/-} mice. These observations support development of therapies suppressing the Siglec-15 function to treat bone loss diseases, such as osteoporosis. In addition, a phenotype restricted to skeletal tissues may mean such therapies have fewer adverse effects on other organs or tissues.

In femoral trabecular bone, both osteoblast surface and bone formation rate per unit bone surface were reduced by Siglec-15 deficiency, indicating a possible role of the gene in osteoblast regulation as well. However, preliminary RT-PCR examinations detected no Siglec-15 expression in murine osteoblast lineage cells, such as ST2 and MC3T3-E1, even when they were cultured under differentiation-inducing conditions. In addition, anti-Siglec-15 antibody, which has a potential to inhibit osteoclast

differentiation, did not affect osteoblastic differentiation *in vitro* when determined by alkaline phosphatase activity in the cells. Although I need to assess the osteogenic capacity of *Siglec15*^{-/-} osteoprogenitor cells to make a conclusion, those preliminary results suggest a low possibility of a direct involvement of Siglec-15 in osteoblast regulation. Instead, reduction in osteoblast number and the bone formation rate observed in the *Siglec15*^{-/-} mice could be accounted for by considering the secondary effect resulting from reduced bone resorption based on the functional coupling concept in bone formation and resorption.

Although the osteopetrotic phenotype of trabecular bone was similar in the male and female *Siglec15*^{-/-} mice, increased bone mass was detected by pQCT and histomorphometrical analyses in cortical bone of the femoral midshaft in the female mice. Interestingly, femoral labeled periosteal surface per unit bone surface increased in the female mutant mice, suggesting that enhanced bone formation partly contributes to increased cortical bone mass. Increased serum osteocalcin levels in the female *Siglec15*^{-/-} mice support this idea, as approximately 80% of bone in the entire body comprises cortical bone [51]. However, enhanced cortical bone formation provokes a further question when contrasted with trabecular bone, where osteoblast surface and bone formation rate were reduced. I do not know why morphological changes in cortical bone differed between male and female mutant mice, nor why bone formation differed between femoral trabecular and cortical bone in female mutants. The molecular mechanisms responsible for the bone-sparing effects of sex steroids (estrogens and androgens) vary as a function of gender, skeletal site, and bone compartment [52, 53], which could provide insight into these differences.

Siglec-15 reportedly associates with the DAP12 adaptor molecule [29], deficiency of which in mice is known to cause mild osteopetrosis [24, 25]. Comparing the skeletal phenotype in the *Siglec15^{-/-}* mice with DAP12-deficient (*DAP12^{-/-}*) mice, we find many similarities. Both mutant mice grow normally without gross skeletal abnormalities, while exhibiting markedly increased trabecular bone. Micro-CT and histological images of trabecular bone in the two mutants are very alike. Another commonality is that the impact of genetic deficiency on osteoclast development differs *in vivo* and *in vitro*. Reportedly, osteoclast number and morphology in the *DAP12^{-/-}* mice were not significantly different from wild type mice, while impaired osteoclast formation was evident *in vitro* [24]. Similarly, in the *Siglec15^{-/-}* mice, TRAP-positive osteoclasts in the tibial metaphysis were indistinguishable from those of wild type mice, but BMM differentiation into osteoclasts was impaired *in vitro*, evident in reduced induction of cellular TRAP activity in response to RANKL or TNF- α . These observations suggest that Siglec-15 mediates cellular signals through interaction with DAP12 in osteoclasts, positively regulating cell differentiation and/or function. Although another DAP12-associated receptor, TREM-2, is considered the principal partner of DAP12 in osteoclasts, its deficiency in mice reportedly caused accelerated osteoclastogenesis *in vitro* without osteopetrosis *in vivo*, in contrast to DAP12 deficiency [54]. Taken together, my results suggest that the Siglec-15/DAP12 complex mediates the signals required for proper osteoclastogenesis more dominantly than the TREM-2/DAP12 complex in mice. Furthermore, the differences between *in vivo* and *in vitro* osteoclast formation may be accounted for by speculating that the *Siglec15^{-/-}* osteoclasts is capable to differentiate *in vivo* via signaling pathways mediated by other ITAM-bearing adaptors, such as FcR γ ; it

was suggested that ITAM-bearing adaptors can functionally compensate for each other [18, 19]. Recently, Ishida-Kitagawa et al. demonstrated the importance of Siglec-15/DAP12-mediated signaling in functional osteoclast formation using chimeras of these proteins *in vitro* [55]. Their results support the relevance of this signaling pathway to *in vivo* osteoclastogenesis.

In this study, I generated *Siglec15*^{-/-} mice, which developed mild osteopetrosis resulting from impaired bone resorption. My findings suggest that Siglec-15 functions in the regulation of osteoclast differentiation and/or function *in vivo*.

General Discussion

To identify novel genes involved in osteoclastogenesis, I searched genes whose expression was specifically up- or down-regulated in giant cell tumor of bone (GCT). Screening by using a human gene expression database identified sialic acid-binding immunoglobulin-like lectin 15 (Siglec-15) as one of the genes markedly overexpressed in GCT. The mRNA expression level of Siglec-15 increased in association with osteoclast differentiation induced by the receptor activator of nuclear factor κ B ligand (RANKL) in both mouse and human culture systems. Furthermore, treatment of mouse and human osteoclast precursors with polyclonal antibody against Siglec-15 markedly inhibited their maturation. These results suggest that Siglec-15 induced by RANKL through the receptor activator of nuclear factor κ B (RANK) is critically involved in osteoclastogenesis (Fig. 10). Following completion of the current study, Ishida-Kitagawa et al. also reported the importance of Siglec-15 in mouse osteoclastogenesis regulation [55]. They identified Siglec-15 as a gene induced by the nuclear factor of activated T-cells, cytoplasmic, calcineurin-dependent 1 (NFATc1), a key transcription factor for osteoclastogenesis. They also confirmed the inhibitory effect of anti-Siglec-15 polyclonal antibody on the osteoclast differentiation and function in a mouse bone marrow-derived monocyte/macrophage (BMM) culture system. In addition, when Siglec-15 expression was knocked down in mouse BMM by infection with retroviral vectors encoding short hairpin RNA specific for Siglec-15, fewer multinucleated cells developed even in the presence of RANKL, and those multinucleated cells were morphologically contracted with disordered actin-ring formation [55]. These changes were accompanied by significantly reduced bone

resorption. Most of their results were consistent with those of my current study, and support the concept that Siglec-15 plays a critical role in functional osteoclast formation.

The Siglec-15-deficient mice (*Siglec15^{-/-}*) showed increased trabecular bone mass in lumbar vertebrae and metaphyseal regions of the femur and tibia, causing mild osteopetrosis. Of note, there were no changes in major organs and tissues other than skeletal tissues according to the pathological examinations at 18 weeks of age. These results suggest that Siglec-15 plays a role specifically in osteoclast physiology. Kameda et al. independently generated Siglec-15-deficient mice and reported similar phenotype characteristics to those of the current study [56]. Their *Siglec15^{-/-}* mice were fertile, showed no significant abnormalities in appearance, and grew normally until at least 12 months of age. Increase in the trabecular bone was apparent at the proximal tibia and L5 vertebra as determined by micro-CT measurement. The authors also analyzed histologic sections of proximal tibia from 9-week old *Siglec15^{-/-}* mice and found that the multinucleated osteoclasts at the secondary spongiosa were small and did not spread on the bone surface, implying that Siglec-15 deficiency leads to defective osteoclast development. Their results indicate the physiological role of Siglec-15 in osteoclast differentiation and function, and strongly support the validity of the results in my current study.

The present study contributes three important elements to our understanding of Siglec-15 as a potential therapeutic target for the treatment of metabolic bone diseases. First, dysfunction of Siglec-15 led to a defect in bone resorption and the consequent increase in bone mass *in vivo*. Second, anti-Siglec-15 antibody inhibited human

osteoclast formation *in vitro*, providing the concept that antibody medication might be effective in clinical use. Finally, a phenotype restricted to skeletal tissues in Siglec-15-deficient mice suggests that therapies suppressing Siglec-15 function may have fewer adverse effects on other organs or tissues. Recently, Stuible et al. developed a monoclonal antibody suppressive to Siglec-15, and reported the effect of the antibody on bone mass in young (4-week old) normal mice [57]. Treatment with anti-Siglec-15 antibody (intraperitoneally injected at 10 mg/kg, twice a week for 4 weeks) led to an increase in bone mineral density at the femur, tibia and lumbar spine. In another report, *Siglec15^{-/-}* mice were ovariectomized and examined for estrogen deficiency-induced bone loss [58]. The *Siglec15^{-/-}* mice showed resistance to bone loss compared to wild-type mice, suggesting that Siglec-15 is involved in estrogen deficiency-induced bone loss. These studies in combination support the notion that anti-Siglec-15 antibody is a potential therapeutic agent for postmenopausal osteoporosis. However, a direct *in vivo* study using a pathological animal model needs to be conducted to confirm the efficacy of anti-Siglec-15 antibody. In addition to postmenopausal osteoporosis, any other bone diseases related to increased osteoclast activity can be considered as target indications for anti-Siglec-15 antibody therapy. For example, the most recent study demonstrated that Siglec-15-deficient mice showed resistance to periarticular bone loss compared to wild-type mice under a condition of antigen-induced arthritis [59], suggesting that Siglec-15 blockage may be effective for reducing periarticular bone loss in rheumatoid arthritis.

Clarifying the signal transduction pathways is a key to understand the physiological role of Siglec-15 in the osteoclast regulation. The question can be divided into two

parts—what activates Siglec-15 (input signal), and how does Siglec-15 mediate the signal intracellularly (output signal). Regarding the input signal, it was reported that Siglec-15 preferentially recognizes Neu5Ac α 2-6GalNAc α -structures, and an arginine residue (R143) in the V-set domain is responsible for the binding [29]. Kameda et al. constructed a point mutant of Siglec-15 (R143A), in which glycan-binding ability is lost, and transfected to *Siglec15*^{-/-} BMM [56]. Unlike wild-type Siglec-15, the R143A mutant was unable to ameliorate the impaired multinuclear osteoclast formation in *Siglec15*^{-/-} cells. Their results suggest that the ligand binding is needed for Siglec-15 to stimulate development of functional osteoclasts (Fig. 10). Although the intrinsic ligand for Siglec-15 has yet to be identified, we can assume that the putative ligand is expressed on osteoclast-lineage cells themselves based on the following two experimental facts. First, clonal RAW264.7 cells without any stromal cells or osteoblasts could differentiate into mature osteoclasts in the presence of RANKL, and anti-Siglec-15 antibody inhibited that differentiation. Second, a previous study showed that sialidase treatment of mouse BMM inhibited RANKL-induced formation of multinucleated osteoclasts [40], suggesting that desialylation inactivated the putative Siglec-15 ligand expressed on the cell surface. Regarding intracellular signal transduction, it has been demonstrated that Siglec-15 cooperates with DAP12 in the osteoclast regulation [55-57]. DAP12 was reportedly detected in protein complexes precipitated with anti-Siglec-15 antibody, and likewise, anti-DAP12 antibody precipitated Siglec-15 protein in RAW264.7 cells which differentiated into osteoclasts [57]. Further, in mouse BMM in which Siglec-15 expression was knocked down, introducing a mutant of Siglec-15 lacking the DAP12-interacting transmembrane lysine

residue did not ameliorate the defect in osteoclast formation in contrast to wild-type protein [55]. In light of the known role and mechanism of action of DAP12 in osteoclast regulation [18, 20], it is assumed that Siglec-15 regulates osteoclast development in concert with RANK/RANKL signaling (Fig. 10). DAP12 reportedly regulates osteoclast differentiation by modulating RANKL/RANK-mediated calcium signaling, which leads to the induction of NFATc1 [18]. However, it was reported that the difference in RANKL-induced calcium oscillations between wild-type and *Siglec15*^{-/-} BMM was slight, suggesting that Siglec-15 is not crucial for calcium signaling during osteoclast development [56]. DAP12 triggers the activation of Syk, a nonreceptor tyrosine kinase, and subsequent multiple signaling pathways which modulate the differentiation and cytoskeletal organization of osteoclasts [18, 60-62]. Further studies are required to elucidate the responsive downstream signaling pathways of the Siglec-15/DAP12 complex, which would lead to better understanding of the role of Siglec-15 in the biology of osteoclasts. Exploring the intrinsic ligand for Siglec-15 has a profound significance for that purpose.

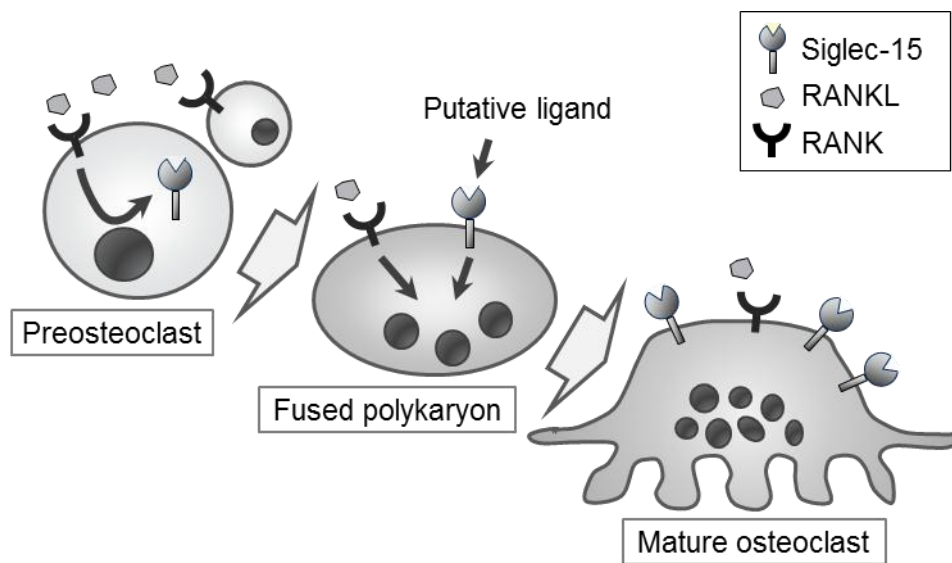


Fig. 10. Model of the functional role of Siglec-15 in osteoclast formation. Siglec-15 induced by RANKL/RANK signaling promotes osteoclast maturation by cooperating with RANKL/RANK signaling cascades. Binding of Siglec-15 to the putative ligand is supposed to be essential for its activation.

Acknowledgements

I would like to express my deep gratitude to Prof. Kazuichi Sakamoto (Faculty of Life and Environmental Sciences, University of Tsukuba) for being in charge of this dissertation, and for his valuable guidance and encouragement.

Also, I would like to express my sincere gratitude to Prof. Osamu Numata (University of Tsukuba), Prof. Tomoki Chiba (University of Tsukuba) and Prof. Hitoshi Miyazaki (University of Tsukuba) for their appropriate advice during the preparation of this dissertation.

Further, I wish to express my sincere gratitude to Dr. Seiichiro Kumakura (Vice President, Biological Research Laboratories, Daiichi Sankyo Co., Ltd) for giving me the opportunity to carry out this study and for offering the appropriate advice.

Also, I am greatly indebted to Dr. Eisuke Tsuda and Dr. Chie Fukuda (Daiichi Sankyo) for their encouragement and helpful guidance in my research work.

Acknowledgements are also made to Mrs. Akiko Okada, Dr. Takehiro Hirai and Dr. Naoyuki Maeda (Daiichi Sankyo) for their kind cooperation and advice in my research work.

Finally, I would like to thank my coworkers at Biological Research Laboratories of Daiichi Sankyo, for their encouragement during the preparation of this dissertation.

References

- [1] Raggatt LJ, Partridge NC. Cellular and molecular mechanisms of bone remodeling. *J Biol Chem* 2010, 285: 25103-25108.
- [2] Raisz LG. Pathogenesis of osteoporosis: concepts, conflicts, and prospects. *J Clin Invest* 2005, 115: 3318-3325.
- [3] Clinician's guide to prevention and treatment of osteoporosis. National Osteoporosis Foundation 2013.
- [4] Kawai M, Modder UI, Khosla S, Rosen CJ. Emerging therapeutic opportunities for skeletal restoration. *Nat Rev Drug Discov* 2011, 10: 141-156.
- [5] Russell RG, Xia Z, Dunford JE, Oppermann U, Kwaasi A, Hulley PA, Kavanagh KL, Triffitt JT, Lundy MW, Phipps RJ, Barnett BL, Coxon FP, Rogers MJ, Watts NB, Ebtino FH. Bisphosphonates: an update on mechanisms of action and how these relate to clinical efficacy. *Ann N Y Acad Sci* 2007, 1117: 209-257.
- [6] Khan AA, Morrison A, Hanley DA, Felsenberg D, McCauley LK, O'Ryan F, Reid IR, Ruggiero SL, Taguchi A, Tetradis S, Watts NB, Brandi ML, Peters E, Guise T, Eastell R, Cheung AM, Morin SN, Masri B, Cooper C, Morgan SL, Obermayer-Pietsch B, Langdahl BL, Al Dabagh R, Davison KS, Kendler DL, Sandor GK, Josse RG, Bhandari M, El Rabbany M, Pierroz DD, Sulimani R, Saunders DP, Brown JP, Compston J. Diagnosis and management of osteonecrosis of the jaw: a systematic review and international consensus. *J Bone Miner Res* 2015, 30: 3-23.
- [7] Reid IR, Cornish J. Epidemiology and pathogenesis of osteonecrosis of the jaw. *Nat Rev Rheumatol* 2012, 8: 90-96.

- [8] Saita Y, Ishijima M, Kaneko K. Atypical femoral fractures and bisphosphonate use: current evidence and clinical implications. *Ther Adv Chronic Dis* 2015, 6: 185-193.
- [9] Park-Wyllie LY, Mamdani MM, Juurlink DN, Hawker GA, Gunraj N, Austin PC, Whelan DB, Weiler PJ, Laupacis A. Bisphosphonate use and the risk of subtrochanteric or femoral shaft fractures in older women. *JAMA* 2011, 305: 783-789.
- [10] Edwards JR, Mundy GR. Advances in osteoclast biology: old findings and new insights from mouse models. *Nat Rev Rheumatol* 2011, 7: 235-243.
- [11] Taichman RS, Emerson SG. The role of osteoblasts in the hematopoietic microenvironment. *Stem Cells* 1998, 16: 7-15.
- [12] Takahashi N, Akatsu T, Udagawa N, Sasaki T, Yamaguchi A, Moseley JM, Martin TJ, Suda T. Osteoblastic cells are involved in osteoclast formation. *Endocrinology* 1988, 123: 2600-2602.
- [13] Udagawa N, Takahashi N, Akatsu T, Sasaki T, Yamaguchi A, Kodama H, Martin TJ, Suda T. The bone marrow-derived stromal cell lines MC3T3-G2/PA6 and ST2 support osteoclast-like cell differentiation in cocultures with mouse spleen cells. *Endocrinology* 1989, 125: 1805-1813.
- [14] Nakagawa N, Kinoshita M, Yamaguchi K, Shima N, Yasuda H, Yano K, Morinaga T, Higashio K. RANK is the essential signaling receptor for osteoclast differentiation factor in osteoclastogenesis. *Biochem Biophys Res Commun* 1998, 253: 395-400.
- [15] Yasuda H, Shima N, Nakagawa N, Yamaguchi K, Kinoshita M, Mochizuki S,

- Tomoyasu A, Yano K, Goto M, Murakami A, Tsuda E, Morinaga T, Higashio K, Udagawa N, Takahashi N, Suda T. Osteoclast differentiation factor is a ligand for osteoprotegerin/osteoclastogenesis-inhibitory factor and is identical to TRANCE/RANKL. *Proc Natl Acad Sci USA* 1998, 95: 3597-3602.
- [16] Lacey DL, Timms E, Tan HL, Kelley MJ, Dunstan CR, Burgess T, Elliott R, Colombero A, Elliott G, Scully S, Hsu H, Sullivan J, Hawkins N, Davy E, Capparelli C, Eli A, Qian YX, Kaufman S, Sarosi I, Shalhoub V, Senaldi G, Guo J, Delaney J, Boyle WJ. Osteoprotegerin ligand is a cytokine that regulates osteoclast differentiation and activation. *Cell* 1998, 93: 165-176.
- [17] Takayanagi H, Kim S, Koga T, Nishina H, Isshiki M, Yoshida H, Saiura A, Isobe M, Yokochi T, Inoue J, Wagner EF, Mak TW, Kodama T, Taniguchi T. Induction and activation of the transcription factor NFATc1 (NFAT2) integrate RANKL signaling in terminal differentiation of osteoclasts. *Dev Cell* 2002, 3: 889-901.
- [18] Koga T, Inui M, Inoue K, Kim S, Suematsu A, Kobayashi E, Iwata T, Ohnishi H, Matozaki T, Kodama T, Taniguchi T, Takayanagi H, Takai T. Costimulatory signals mediated by the ITAM motif cooperate with RANKL for bone homeostasis. *Nature* 2004, 428: 758-763.
- [19] Mocsai A, Humphrey MB, Van Ziffle JA, Hu Y, Burghardt A, Spusta SC, Majumdar S, Lanier LL, Lowell CA, Nakamura MC. The immunomodulatory adapter proteins DAP12 and Fc receptor gamma-chain (FcRgamma) regulate development of functional osteoclasts through the Syk tyrosine kinase. *Proc Natl Acad Sci USA* 2004, 101: 6158-6163.
- [20] Humphrey MB, Lanier LL, Nakamura MC. Role of ITAM-containing adapter

proteins and their receptors in the immune system and bone. *Immunol Rev* 2005, 208: 50-65.

- [21] Paloneva J, Kestila M, Wu J, Salminen A, Bohling T, Ruotsalainen V, Hakola P, Bakker AB, Phillips JH, Pekkarinen P, Lanier LL, Timonen T, Peltonen L. Loss-of-function mutations in TYROBP (DAP12) result in a presenile dementia with bone cysts. *Nat Genet* 2000, 25: 357-361.
- [22] Paloneva J, Manninen T, Christman G, Hovanes K, Mandelin J, Adolfsson R, Bianchin M, Bird T, Miranda R, Salmaggi A, Tranebjaerg L, Konttinen Y, Peltonen L. Mutations in two genes encoding different subunits of a receptor signaling complex result in an identical disease phenotype. *Am J Hum Genet* 2002, 71: 656-662.
- [23] Kondo T, Takahashi K, Kohara N, Takahashi Y, Hayashi S, Takahashi H, Matsuo H, Yamazaki M, Inoue K, Miyamoto K, Yamamura T. Heterogeneity of presenile dementia with bone cysts (Nasu-Hakola disease): three genetic forms. *Neurology* 2002, 59: 1105-1107.
- [24] Kaifu T, Nakahara J, Inui M, Mishima K, Momiyama T, Kaji M, Sugahara A, Koito H, Ujike-Asai A, Nakamura A, Kanazawa K, Tan-Takeuchi K, Iwasaki K, Yokoyama WM, Kudo A, Fujiwara M, Asou H, Takai T. Osteopetrosis and thalamic hypomyelinoses with synaptic degeneration in DAP12-deficient mice. *J Clin Invest* 2003, 111: 323-332.
- [25] Humphrey MB, Ogasawara K, Yao W, Spusta SC, Daws MR, Lane NE, Lanier LL, Nakamura MC. The signaling adapter protein DAP12 regulates multinucleation during osteoclast development. *J Bone Miner Res* 2004, 19: 224-234.

- [26] Werner M. Giant cell tumour of bone: morphological, biological and histogenetical aspects. *Int Orthop* 2006, 30: 484-489.
- [27] Crocker PR, Paulson JC, Varki A. Siglecs and their roles in the immune system. *Nat Rev Immunol* 2007, 7: 255-266.
- [28] von Gunten S, Bochner BS. Basic and clinical immunology of Siglecs. *Ann N Y Acad Sci* 2008, 1143: 61-82.
- [29] Angata T, Tabuchi Y, Nakamura K, Nakamura M. Siglec-15: an immune system Siglec conserved throughout vertebrate evolution. *Glycobiology* 2007, 17: 838-846.
- [30] Macauley MS, Crocker PR, Paulson JC. Siglec-mediated regulation of immune cell function in disease. *Nat Rev Immunol* 2014, 14: 653-666.
- [31] Hofbauer LC, Schoppet M. Clinical implications of the osteoprotegerin/RANKL/RANK system for bone and vascular diseases. *JAMA* 2004, 292: 490-495.
- [32] Lewiecki EM. Denosumab for joints and bones. *Curr Rheumatol Rep* 2009, 11: 196-201.
- [33] Roux S, Amazit L, Meduri G, Guiochon-Mantel A, Milgrom E, Mariette X. RANK (receptor activator of nuclear factor kappa B) and RANK ligand are expressed in giant cell tumors of bone. *Am J Clin Pathol* 2002, 117: 210-216.
- [34] Huang L, Xu J, Wood DJ, Zheng MH. Gene expression of osteoprotegerin ligand, osteoprotegerin, and receptor activator of NF-kappaB in giant cell tumor of bone: possible involvement in tumor cell-induced osteoclast-like cell formation. *Am J Pathol* 2000, 156: 761-767.

- [35] Atkins GJ, Haynes DR, Graves SE, Evdokiou A, Hay S, Bouralexis S, Findlay DM. Expression of osteoclast differentiation signals by stromal elements of giant cell tumors. *J Bone Miner Res* 2000, 15: 640-649.
- [36] Skubitz KM, Cheng EY, Clohisy DR, Thompson RC, Skubitz AP. Gene expression in giant-cell tumors. *J Lab Clin Med* 2004, 144: 193-200.
- [37] Krogh A, Larsson B, von Heijne G, Sonnhammer EL. Predicting transmembrane protein topology with a hidden Markov model: application to complete genomes. *J Mol Biol* 2001, 305: 567-580.
- [38] Hsu H, Lacey DL, Dunstan CR, Solovyev I, Colombero A, Timms E, Tan HL, Elliott G, Kelley MJ, Sarosi I, Wang L, Xia XZ, Elliott R, Chiu L, Black T, Scully S, Capparelli C, Morony S, Shimamoto G, Bass MB, Boyle WJ. Tumor necrosis factor receptor family member RANK mediates osteoclast differentiation and activation induced by osteoprotegerin ligand. *Proc Natl Acad Sci USA* 1999, 96: 3540-3545.
- [39] Takahashi N, Yamana H, Yoshiki S, Roodman GD, Mundy GR, Jones SJ, Boyde A, Suda T. Osteoclast-like cell formation and its regulation by osteotropic hormones in mouse bone marrow cultures. *Endocrinology* 1988, 122: 1373-1382.
- [40] Takahata M, Iwasaki N, Nakagawa H, Abe Y, Watanabe T, Ito M, Majima T, Minami A. Sialylation of cell surface glycoconjugates is essential for osteoclastogenesis. *Bone* 2007, 41: 77-86.
- [41] Gallagher JC. Advances in bone biology and new treatments for bone loss. *Maturitas* 2008, 60: 65-69.
- [42] Tolar J, Teitelbaum SL, Orchard PJ. Osteopetrosis. *N Engl J Med* 2004, 351:

2839-2849.

- [43] Segovia-Silvestre T, Neutzsky-Wulff AV, Sorensen MG, Christiansen C, Bollerslev J, Karsdal MA, Henriksen K. Advances in osteoclast biology resulting from the study of osteopetrotic mutations. *Hum Genet* 2009, 124: 561-577.
- [44] Leibbrandt A, Penninger JM. RANK/RANKL: regulators of immune responses and bone physiology. *Ann N Y Acad Sci* 2008, 1143: 123-150.
- [45] Barka T, Anderson PJ. Histochemical methods for acid phosphatase using hexazonium pararosanilin as coupler. *J Histochem Cytochem* 1962, 10: 741-753.
- [46] Parfitt AM, Drezner MK, Glorieux FH, Kanis JA, Malluche H, Meunier PJ, Ott SM, Recker RR. Bone histomorphometry: standardization of nomenclature, symbols, and units. Report of the ASBMR Histomorphometry Nomenclature Committee. *J Bone Miner Res* 1987, 2: 595-610.
- [47] Dougall WC, Glaccum M, Charrier K, Rohrbach K, Brasel K, De Smedt T, Daro E, Smith J, Tometsko ME, Maliszewski CR, Armstrong A, Shen V, Bain S, Cosman D, Anderson D, Morrissey PJ, Peschon JJ, Schuh J. RANK is essential for osteoclast and lymph node development. *Genes Dev* 1999, 13: 2412-2424.
- [48] Johnson RS, Spiegelman BM, Papaioannou V. Pleiotropic effects of a null mutation in the *c-fos* proto-oncogene. *Cell* 1992, 71: 577-586.
- [49] Grigoriadis AE, Wang ZQ, Cecchini MG, Hofstetter W, Felix R, Fleisch HA, Wagner EF. *c-Fos*: a key regulator of osteoclast-macrophage lineage determination and bone remodeling. *Science* 1994, 266: 443-448.
- [50] Azuma Y, Kaji K, Katogi R, Takeshita S, Kudo A. Tumor necrosis factor-alpha induces differentiation of and bone resorption by osteoclasts. *J Biol Chem* 2000,

275: 4858-4864.

- [51] Barrett KE, Brooks H, Boitano S, Barman SM. Ganong's review of medical physiology, 23rd eddition. New York, NY: McGraw-Hill Medical; 2009.
- [52] Frenkel B, Hong A, Baniwal SK, Coetzee GA, Ohlsson C, Khalid O, Gabet Y. Regulation of adult bone turnover by sex steroids. *J Cell Physiol* 2010, 224: 305-310.
- [53] Nakamura T, Imai Y, Matsumoto T, Sato S, Takeuchi K, Igarashi K, Harada Y, Azuma Y, Krust A, Yamamoto Y, Nishina H, Takeda S, Takayanagi H, Metzger D, Kanno J, Takaoka K, Martin TJ, Chambon P, Kato S. Estrogen prevents bone loss via estrogen receptor alpha and induction of Fas ligand in osteoclasts. *Cell* 2007, 130: 811-823.
- [54] Colonna M, Turnbull I, Klesney-Tait J. The enigmatic function of TREM-2 in osteoclastogenesis. *Adv Exp Med Biol* 2007, 602: 97-105.
- [55] Ishida-Kitagawa N, Tanaka K, Bao X, Kimura T, Miura T, Kitaoka Y, Hayashi K, Sato M, Maruoka M, Ogawa T, Miyoshi J, Takeya T. Siglec-15 protein regulates formation of functional osteoclasts in concert with DNAX-activating protein of 12 kDa (DAP12). *J Biol Chem* 2012, 287: 17493-17502.
- [56] Kameda Y, Takahata M, Komatsu M, Mikuni S, Hatakeyama S, Shimizu T, Angata T, Kinjo M, Minami A, Iwasaki N. Siglec-15 regulates osteoclast differentiation by modulating RANKL-induced phosphatidylinositol 3-kinase/Akt and Erk pathways in association with signaling Adaptor DAP12. *J Bone Miner Res* 2013, 28: 2463-2475.
- [57] Stuiblé M, Moraitis A, Fortin A, Saragosa S, Kalbakji A, Filion M, Tremblay GB.

Mechanism and function of monoclonal antibodies targeting siglec-15 for therapeutic inhibition of osteoclastic bone resorption. *J Biol Chem* 2014, 289: 6498-6512.

- [58] Kameda Y, Takahata M, Mikuni S, Shimizu T, Hamano H, Angata T, Hatakeyama S, Kinjo M, Iwasaki N. Siglec-15 is a potential therapeutic target for postmenopausal osteoporosis. *Bone* 2015, 71: 217-226.
- [59] Shimizu T, Takahata M, Kameda Y, Endo T, Hamano H, Hiratsuka S, Ota M, Iwasaki N. Sialic acid-binding immunoglobulin-like lectin 15 (Siglec-15) mediates periarticular bone loss, but not joint destruction, in murine antigen-induced arthritis. *Bone* 2015, 79: 65-70.
- [60] Faccio R, Teitelbaum SL, Fujikawa K, Chappel J, Zallone A, Tybulewicz VL, Ross FP, Swat W. Vav3 regulates osteoclast function and bone mass. *Nat Med* 2005, 11: 284-290.
- [61] Mao D, Epple H, Uthgenannt B, Novack DV, Faccio R. PLCgamma2 regulates osteoclastogenesis via its interaction with ITAM proteins and GAB2. *J Clin Invest* 2006, 116: 2869-2879.
- [62] Reeve JL, Zou W, Liu Y, Maltzman JS, Ross FP, Teitelbaum SL. SLP-76 couples Syk to the osteoclast cytoskeleton. *J Immunol* 2009, 183: 1804-1812.